

Elsevier Editorial System(tm) for Earth and
Planetary Science Letters

Manuscript Draft

Manuscript Number: EPSL-D-19-01080R3

Title: Into the deep and beyond: carbon and nitrogen subduction recycling
in secondary peridotites

Article Type: Letters

Keywords: Carbon; Nitrogen, Subduction zone; Carbon isotope; blue boron
diamonds; Serpentinites

Corresponding Author: Dr. Enrico Cannà, Ph.D.

Corresponding Author's Institution: University of Milan

First Author: Enrico Cannà, Ph.D.

Order of Authors: Enrico Cannà, Ph.D.; Massimo Tiepolo, PhD; Gray
Bebout, PhD; Marco Scambelluri, PhD

Abstract: Understanding the volatile cycles at convergent margins is fundamental to unravel the Earth's evolution from primordial time to present. The assessment of fluid-mobile and incompatible element uptake in serpentinites via interaction with seawater and subduction-zone fluids is central to evaluate the global cycling of the above elements in the Earth's mantle produces chlorite-bearing and, at higher temperatures, garnet-bearing secondary peridotites (i.e., metaperidotites). Here, we focus on the carbon (C), nitrogen (N) and C isotope compositions of chlorite harzburgites and garnet peridotites deriving from subduction-zone dehydration of former oceanic dehydration of serpentinite (Cima di Gagnone, Swiss Central Alps) with the aim of evaluating the contribution of these rocks to the global C-N cycling. These ultramafic rocks, enclosed as lenses in a metasedimentary mélange, represent the destabilization of antigorite and chlorite at high-pressure/temperature (P/T) along a slab-mantle interface. Chlorite- and garnet-bearing rocks have similar ranges in C concentration ($[C] = 210 - 2465$ ppm and $304 - 659$ ppm, respectively), with one magnesite-bearing chlorite harzburgite hosting 11000 ppm C. The average N concentrations ($[N]$) of the garnet peridotites (54 ± 15 ppm, one standard deviation indicated) are higher than those of the chlorite harzburgites (29 ± 6 ppm). The $\delta^{13}C$ of total C (TC) and total organic C (TOC) values of the Gagnone metaperidotites range from -12.2 to -17.8 ‰ and from -27.8 to -26.8 ‰, respectively, excluding the magnesite-bearing chlorite harzburgites with higher values of -7.2 ‰ (TC) and -21.2 ‰ (TOC). The $[C]$ of these rocks are comparable to those of serpentinites from modern and ancient oceanic environments and with $[C]$ of high-P serpentinites. However, the lack of preserved serpentinite precursors makes it difficult to determine whether release of H₂O during high-P breakdown of antigorite and chlorite is coupled with significant C release to fluids. The $\delta^{13}C$ values appear to reflect mixing between seawater-derived carbonate and a reduced C source and a contribution from the host metasedimentary rocks ($[C] = 301$ ppm; $[N] = 33$ ppm; TC $\delta^{13}C = -24.4$ ‰; TOC $\delta^{13}C = -27.0$ ‰) cannot be completely excluded. The C-O isotope composition of the carbonate in magnesite-bearing chlorite harzburgites is compatible with progressive

devolatilization at oxidized conditions, whereas the signatures of the majority of the other Gagnone samples appear to reflect different degree of interaction with sedimentary fluids. The [N] of the Gagnone metaperidotites are higher than those of oceanic and subducted serpentinites and show a range similar to that of high-P antigorite-serpentinites from mantle wedges. This enrichment is compatible with fluid-mediated chemical exchange with the surrounding metasedimentary rocks leading to strong modification of the Gagnone metaperidotites' geochemistry during prograde subduction along the slab-mantle interface. Comparing the $\delta^{13}\text{C}$ data reported in this study with published $\delta^{13}\text{C}$ values for diamonds, we suggest that the volatile recycling via Gagnone-like metaperidotites in subduction zones could contribute to deep-Earth diamond genesis and in particular to the formation of blue boron (B)-bearing diamonds. Our results highlight that the subduction of secondary peridotites evolved along the slab-mantle interface is a viable mechanism to inject volatiles into the deep mantle, particularly in hotter geothermal regimes such as the ones active during the early Earth's history.

Into the deep and beyond: carbon and nitrogen subduction recycling in secondary peridotites

Cannaò E.^a, Tiepolo M.^a, Bebout G. E.^b, Scambelluri M.^c

*^aDipartimento di Scienze della Terra “A. Desio”, Università di Milano, Via Botticelli 23, 21133 Milano,
Italy*

^bDepartment of Earth and Environmental Sciences, Lehigh University, Bethlehem, PA 18015, USA

*^cDipartimento di Scienze della Terra, dell’Ambiente e della Vita, Università di Genova, C.so Europa 26,
16132 Genova, Italy*

corresponding author: enrico.cannaio@unimi.it

1 **Abstract**

2 Understanding the volatile cycles at convergent margins is fundamental to unravel the Earth's
3 evolution from primordial time to present. The assessment of fluid-mobile and incompatible element uptake
4 in serpentinites via interaction with seawater and subduction-zone fluids is central to evaluate the global
5 cycling of the above elements in the Earth's mantle produces chlorite-bearing and, at higher temperatures,
6 garnet-bearing secondary peridotites (i.e., metaperidotites). Here, we focus on the carbon (C), nitrogen (N)
7 and C isotope compositions of chlorite harzburgites and garnet peridotites deriving from subduction-zone
8 dehydration of former oceanic dehydration of serpentinite (Cima di Gagnone, Swiss Central Alps) with the
9 aim of evaluating the contribution of these rocks to the global C-N cycling. These ultramafic rocks, enclosed
10 as lenses in a metasedimentary *mélange*, represent the destabilization of antigorite and chlorite at high-
11 pressure/temperature (*P/T*) along a slab-mantle interface. Chlorite- and garnet-bearing rocks have similar
12 ranges in C concentration ($[C] = 210 - 2465$ ppm and $304 - 659$ ppm, respectively), with one magnesite-
13 bearing chlorite harzburgite hosting 11000 ppm C. The average N concentrations ($[N]$) of the garnet
14 peridotites (54 ± 15 ppm, one standard deviation indicated) are higher than those of the chlorite harzburgites
15 (29 ± 6 ppm). The $\delta^{13}C$ of total C (TC) and total organic C (TOC) values of the Gagnone metaperidotites
16 range from -12.2 to -17.8 ‰ and from -27.8 to -26.8 ‰, respectively, excluding the magnesite-bearing
17 chlorite harzburgites with higher values of -7.2 ‰ (TC) and -21.2 ‰ (TOC). The $[C]$ of these rocks are
18 comparable to those of serpentinites from modern and ancient oceanic environments and with $[C]$ of high-*P*
19 serpentinites. However, the lack of preserved serpentinite precursors makes it difficult to determine whether
20 release of H₂O during high-*P* breakdown of antigorite and chlorite is coupled with significant C release to
21 fluids. The $\delta^{13}C$ values appear to reflect mixing between seawater-derived carbonate and a reduced C source
22 and a contribution from the host metasedimentary rocks ($[C] = 301$ ppm; $[N] = 33$ ppm; TC $\delta^{13}C = -24.4$ ‰;
23 TOC $\delta^{13}C = -27.0$ ‰) cannot be completely excluded. The C-O isotope composition of the carbonate in
24 magnesite-bearing chlorite harzburgites is compatible with progressive devolatilization at oxidized
25 conditions, whereas the signatures of the majority of the other Gagnone samples appear to reflect different
26 degree of interaction with sedimentary fluids. The $[N]$ of the Gagnone metaperidotites are higher than those
27 of oceanic and subducted serpentinites and show a range similar to that of high-*P* antigorite-serpentinites
28 from mantle wedges. This enrichment is compatible with fluid-mediated chemical exchange with the

29 surrounding metasedimentary rocks leading to strong modification of the Gagnone metaperidotites'
30 geochemistry during prograde subduction along the slab-mantle interface. Comparing the $\delta^{13}\text{C}$ data reported
31 in this study with published $\delta^{13}\text{C}$ values for diamonds, we suggest that the volatile recycling via Gagnone-
32 like metaperidotites in subduction zones could contribute to deep-Earth diamond genesis and in particular to
33 the formation of blue boron (B)-bearing diamonds. Our results highlight that the subduction of secondary
34 peridotites evolved along the slab-mantle interface is a viable mechanism to inject volatiles into the deep
35 mantle, particularly in hotter geothermal regimes such as the ones active during the early Earth's history.

36

37 *Keywords: Carbon; Nitrogen, Subduction zone; Carbon isotope; blue boron diamonds; Serpentinites*

38

39 **1. Introduction**

40 Volatiles largely impact on refertilization and dynamics of the Earth's mantle; therefore, clarifying
41 their deep geochemical cycle improves our understanding of how the interior of our planet evolved through
42 time. Subduction largely governs material flux among Earth's surface reservoirs and mantle and
43 metamorphic reactions and fluid-rock chemical exchange can have considerable impact on the magnitude
44 and geochemical signatures of this flux (e.g., Bebout, 2014; Cannà and Malaspina, 2018 and references
45 therein). The compositions of oceanic island basalts (OIB) are thought to reflect recycling into the lower
46 mantle of either altered oceanic crust (AOC) or AOC plus subordinate sediments/continental crust (e.g.,
47 Hofmann, 2014) and subduction zone metamorphism could modify the major and trace element and isotopic
48 compositions of these rocks during their transit into the deep mantle (e.g., Bebout, 2007). The involvement
49 of formerly serpentinized lithospheric mantle in the genesis of OIB magmas has been recently invoked to
50 explain the high concentrations of water and halogens in OIB basalt glasses (Kendrick et al., 2017). This idea
51 is supported by the isotopic composition of several Alpine high-pressure (*P*) serpentinites investigated by
52 Scambelluri et al. (2019). Smith et al (2018) suggested that devolatilized serpentinites play a role in the
53 genesis of blue boron(B)-bearing diamonds, by conveying large amounts of light elements into the lower
54 mantle. This evidence, together with the nitrogen (N) isotope compositions of early Archean diamonds
55 pointing to deep recycling of exogenic N (Cartigny, 2005), suggests that modern-style plate tectonics might

56 have been active since the Earth's infancy (Smart et al., 2016). If this is true, subduction has likely played a
57 vital role in global volatile cycling over much of Earth's history.

58 Historically, the C and N input into the mantle has largely been attributed to subduction of oceanic
59 (meta)sediments and AOC. Seafloor sedimentary reservoirs enable the injection of both inorganic and
60 organic C, and N of organic origin (e.g., Bebout et al., 2013; Cook-Kollars et al., 2014), whereas seafloor
61 hydrothermal alteration heterogeneously enriches oceanic crust and the lithospheric mantle C largely as
62 carbonates, in addition to sedimentary/organic N contributed via fluid-rock interactions (see Busigny et al.,
63 2005; Li et al., 2007). The subduction of ophiocarbonate horizons represents an adjunctive vector for
64 conveying volatiles into the mantle (e.g., Alt and Teagle, 1999; Collins et al., 2015). Until recently, the
65 contribution of slab hydrated ultramafic rocks (i.e., pure serpentinites) to global C-N flux has been
66 considered less important than that from subducting sedimentary rocks and AOC (Alt et al., 2012a).
67 However, in recent views of subduction (e.g., Bebout and Penniston-Dorland, 2016), serpentinites are
68 regarded as occurring in large hydrated domains along subduction plate interfaces, where they behave as
69 trap-transport-release systems for volatile and incompatible elements (e.g., Guillot et al., 2015; Scambelluri
70 et al., 2019 and references therein). In addition to transferring to depth C acquired on the seafloor, these
71 rocks can trap and transport C released by other subducting rocks experiencing decarbonation and carbonate
72 dissolution (Galvez et al., 2013; Piccoli et al., 2016; Scambelluri et al., 2016; Vitale Brovarone et al., 2017).
73 Thus far, few data on the C (and N) contents of serpentinitized/de-serpentinitized mantle rocks from the slab-
74 mantle interface have been presented in literature (see Schwarzenbach et al., 2018).

75 In this paper, we present C and N concentrations and $\delta^{13}\text{C}$ values of secondary Alpine peridotites
76 (hereafter referred to as metaperidotites) derived from the subduction zone dehydration of serpentinite
77 precursors. These rocks, from Cima di Gagnone (Swiss Central Alps) record two main high-*P* dehydration
78 episodes: the first driven by serpentine breakdown to chlorite, olivine and orthopyroxene and the second
79 involving chlorite breakdown to produce garnet peridotite (Scambelluri et al., 2015). These represent key
80 dehydration reactions accompanied by volatile redistribution between fluids and dehydrated rock residues
81 and are also no-return transformations which cause the densification and deep subduction of large domains
82 of slab (and potentially wedge) materials. Previous petrologic and geochemical studies on the Gagnone
83 metaperidotites show that these rocks record subduction-zone chemical exchange with sedimentary rocks

84 that modified their pre-subduction (seafloor-derived) trace elements and isotopic compositions (Cannaò et
85 al., 2015; Kendrick et al., 2018; Scambelluri et al., 2015, 2014). Here, we propose that the deep subduction
86 of such materials can convey significant amounts of C and N to depths beyond those beneath arcs, affecting
87 the deep-Earth cycling of these elements and potentially contributing to the genesis of some types of
88 diamonds.

89

90 **2. Geological background and samples description**

91 The Cima di Gagnone metaperidotites belong to the Adula-Cima Lunga Unit (Central Alps),
92 representing the southernmost European margin involved in the Alpine orogeny. In this unit, bodies of
93 ultramafic-mafic rocks enclosed in ortho- and para-gneisses recrystallized at eclogite-facies *P-T* conditions
94 during Alpine subduction. According to several authors (Evans et al., 1979; Evans and Trommsdorff, 1978;
95 Meyre et al., 1999), in the Adula-Cima Lunga unit the eclogite *P-T* conditions increase from north (1.2 GPa
96 – 500 °C) to south (2.5 GPa – 850 °C). The Cima di Gagnone ultramafic rocks are exposed in the northern
97 part of the Cima Lunga nappe and correspond to garnet-bearing peridotite and associated chlorite harzburgite
98 formed at 2.5 – 3.0 GPa and 750 – 800 °C (Evans and Trommsdorff, 1978; Scambelluri et al., 2014). Within
99 the chlorite harzburgite, the presence of eclogite and high-*P* metarodingite deriving from MORB-type
100 basaltic/gabbroic dykes (Evans et al., 1979) records a history of oceanic intrusion and hydration/alteration
101 prior to Alpine subduction of the entire Gagnone-rock suite. The Gagnone metaperidotites thus derive from
102 oceanic (or wedge?) serpentinites that experienced complete antigorite-breakdown during the high-*P* stage
103 about 40 Ma ago (Becker, 1993). The occurrence of relict antigorite inclusions inside Ti-clinohumite, and the
104 preservation of primary fluid-related inclusions in metamorphic olivine and garnet (after antigorite and
105 chlorite dehydration, respectively), confirm that this dehydration event affected these rocks (Scambelluri et
106 al., 2015). Metaperidotites show LREE depletion related to mantle melting and reactive melt flow in the
107 oceanic lithosphere, as well as enrichment in fluid-mobile elements (FME: B, As, Sb, U and Th), pointing to
108 multiple oceanic and subduction hydration events (Scambelluri et al., 2014). Their highly radiogenic Sr and
109 Pb isotopic composition and negative $\delta^{11}\text{B}$ indicate prograde-metamorphic interaction with fluids sourced
110 from the host metasedimentary rocks (Cannaò et al., 2015). Enrichment in fluid-mobile element (FME) is a
111 common feature in all eclogite-facies minerals forming the Gagnone ultramafic rocks, implying that the

112 FME additions predate the peak eclogite-facies dehydration. Analyses of halogens and noble gases also
113 highlight the chemical exchange between ultramafic and sedimentary reservoirs (Kendrick et al., 2018).

114 In this study, we analyzed two garnet peridotites and three chlorite harzburgites for all of which
115 detailed and complete descriptions have previously been published (Cannaò et al., 2015; Scambelluri et al.,
116 2015, 2014). The garnet peridotites (samples MG160 and MG161) display an eclogite foliation defined by
117 olivine, ortho- and clinopyroxene, garnet and Mg-hornblende. Former Ti-clinohumite has been replaced by
118 intergrown ilmenite + olivine. Garnet is pokiloblastic, hosting inclusions of pre-eclogitic minerals including
119 orthopyroxene, chlorite, Ca-amphibole and spinel (Scambelluri et al., 2014). The chlorite harzburgites show
120 both foliated (samples MG31 09-06, MG163 09-07) and undeformed textures (samples MG 304 92-1 and 2).
121 The foliation exhibited in some chlorite harzburgites is parallel to the high-*P* foliation in the eclogite and
122 metarodingite bodies. In both deformed and undeformed rock types, olivine, orthopyroxene and chlorite are
123 the major rock-forming minerals, with magnetite, ilmenite and Fe-rich chromite as accessory phases.
124 Fluorine-bearing Ti-clinohumite has been identified in the undeformed rocks only. Sample MG304 92-2
125 contains magnesite with textures indicating equilibration with the high-*P* mineral assemblages. Sample
126 MG163 12-03 is a dunite containing abundant olivine and minor orthopyroxene and chlorite, with magnetite,
127 ilmenite and chromite as accessory minerals. In almost all samples, carbonate-bearing (micro)inclusions
128 have been identified within high-*P* minerals (Scambelluri et al., 2015).

129

130 **3. Methods**

131 Samples selected for this work were previously analyzed for their whole-rock major and trace
132 element concentrations and Sr-Pb and B isotopic compositions (Cannaò et al., 2015; Scambelluri et al.,
133 2014). In this study, ten whole-rock samples of metaperidotites from Gagnone were analyzed for their
134 concentrations of C and N and isotopic compositions of total C, total inorganic C and total organic C (TC,
135 TIC and TOC, respectively). To evaluate the potential exchange with the country rocks, we determined the C
136 (TC) and N concentrations and $\delta^{13}\text{C}$ (TC and TOC) of one sample of paragneiss (Cannaò et al. 2015). Total
137 C, N and TOC results were determined at the Earth Science Department, University of Milan (Italy), using a
138 Thermo Fischer Organic Elemental Analyzer (OEA, Flash2000) coupled to a Thermo Scientific Delta V
139 Advantage mass spectrometer via a ConFlo IV interface. Inorganic (i.e., carbonate) C and O isotope

140 compositions (Total Inorganic Carbon – TIC) were analyzed at the Department of Earth and Environmental
141 Sciences, Lehigh University (USA), using a Finnigan MAT 252 gas mass-spectrometer coupled with a
142 GasBench II system, applying the methods described by Cook-Kollars et al. (2014) and Collins et al. (2015).
143 All data are presented in standard δ -notation and expressed relative to VPDB and VSMOW for $\delta^{13}\text{C}$ and
144 $\delta^{18}\text{O}$, respectively. The complete method details are reported in **Appendix A**.

145

146 **4. Results**

147 Carbon and N concentrations, $\delta^{13}\text{C}$ values (TC, TIC, TOC) and the $\delta^{18}\text{O}$ values (of inorganic
148 carbonate) obtained during this study are reported in **Table 1**. The TC concentrations of metaperidotites
149 range from 210 to 712 ppm, excluding samples MG163 09-07 and MG304 92-2 that show higher C content
150 of 2465 and 10966 ppm, respectively (**Fig. 1A**). TIC ranges from 108 to 372 ppm, excluding the magnesite-
151 bearing sample MG 304 92-2 containing 3300 ppm of TIC. The TOC contents were calculated by simple
152 differences between TC and TIC concentrations and are reported in **Table 1**. Excluding samples MG304 92-
153 2 and MG163 09-07, all TOC concentrations are below 550 ppm, and are comparable to published data for
154 other ultramafic lithologies (e.g., Alt et al. 2012a). Because all samples appear to lack carbonaceous
155 materials based on petrographic investigations, the higher TOC values obtained for the MG304 92-2 and
156 MG163 09-07 rocks suggest either that their TIC concentrations are low due to minor analytical error (i.e.,
157 underestimated TIC) or, alternatively, that minor C contamination occurred during sample preparation for
158 the TC analyses. The average N concentration of metaperidotites is 42 ± 17 ppm; in more detail, the garnet-
159 metaperidotites have higher N (40 – 74 ppm) than the chlorite harzburgites (24 – 38 ppm; **Fig. 1A**).

160 The $\delta^{13}\text{C}$ of the TC and TOC ranges between -17.8 to -12.2‰ and between -27.8 to -26.0‰,
161 respectively, with no significant difference between the garnet- and the chlorite-bearing metaperidotites (**Fig.**
162 **2**). Only the magnesite-bearing chlorite harzburgites sample MG304 92-2 displays less negative $\delta^{13}\text{C}$ value
163 of -7.2 and -21.8‰ for the TC and TOC, respectively.

164 The $\delta^{13}\text{C}$ of the TIC is quite uniform for all samples ($-5.9 \pm 0.5\%$), excluding the chlorite
165 harzburgite MG163 09-07 ($\delta^{13}\text{C}_{\text{TIC}} = -3.5\%$) and the two garnet-bearing metaperidotites MG160 4/8 and
166 MG160 09-10, the later which show more negative values ($\delta^{13}\text{C}_{\text{TIC}} = -8.0$ and -8.4% , respectively; see **Table**
167 **1**). The $\delta^{18}\text{O}_{\text{VSMOW}}$ of the carbonate component differs for the two rock types, being $+22.1 \pm 1.6\%$ for the

168 garnet peridotites and $+17.3 \pm 2.0\%$ for the chlorite harzburgites. The most C-rich chlorite harzburgite
169 samples MG 163 09-07 and MG304 92-2 have $\delta^{18}\text{O}$ values of +12.0 and +7.2‰, respectively, lower than
170 values for C-poor chlorite harzburgites.

171 The one paragneiss sample (MG163 12-17) has relatively low concentrations of C and N (301 and 33
172 ppm, respectively) and its $\delta^{13}\text{C}$ values for TC and TOC are -24.4 and -27.0‰, respectively.

173

174 **5. Discussion**

175 The dataset presented here yields insight regarding the deep recycling of C and N in secondary
176 peridotites evolved along the subduction zone plate interface. In this section, we first compare our results
177 with the C and N concentrations and $\delta^{13}\text{C}$ of serpentinites and deserpentinized ultramafic rocks available in
178 literature (**Figs. 1, 2 and 3**), including those for serpentinites from modern and fossil oceans floor settings
179 and ancient subduction zones (Alt et al., 2012b, 2012a; Delacour et al., 2008; Halama et al., 2012; Philippot
180 et al., 2007; Schwarzenbach et al., 2013). Also, we consider the recently published N measurements for
181 wedge-derived antigorite-serpentinites from the Himalayan Tso Moriri unit (Pagé et al., 2018; **Fig. 3B**). In
182 the final section of the discussion, we attempt to connect the volatile recycling via Gagnone-like
183 metaperidotites to deep diamond genesis, comparing the $\delta^{13}\text{C}$ data reported in this study with published
184 worldwide $\delta^{13}\text{C}$ values of diamonds (**Fig. 5**). Finally, because the subduction of serpentinites and their
185 dehydrated products is a viable mechanism for injecting volatiles and FME into the deep mantle, we explore
186 the potential role of Gagnone-like metaperidotites in contributing to the geochemically anomalous mantle
187 sources of blue boron(B)-bearing diamonds (**Fig. 6**; Smith et al., 2018).

188

189 **5.1. Deep carbon recycling in ultramafic rocks and the $\delta^{13}\text{C}_{\text{TC}}$ anomalies in the mantle**

190 Total C concentrations of oceanic serpentinites are extremely variable (**Figs. 2A, B**) due to the nature
191 of the interaction of mantle rocks exposed on the ocean floor with the inorganic/organic C dissolved in fluids
192 circulating through the oceanic lithosphere (e.g., Delacour et al., 2008, Schwarzenbach et al., 2013). The
193 total C concentrations of the Gagnone metaperidotites are comparable to those of serpentinites from oceanic
194 and subduction zones suites (e.g., Apennine and Iberian margin, Voltri Massif and Almiraz, respectively;
195 **Fig. 1A, 2**). Although the high-*P* serpentinite dehydration during subduction was accompanied by a

196 significant loss of H₂O (**Fig. 3A**), similarity in the C concentrations in the antigorite-serpentinites and
197 chlorite harzburgites from the Almirez ultramafic rock-suite suggests that serpentinite dehydration does not
198 much-affect the C budget of such rocks (Alt et al., 2012a; **Fig. 3A**). Despite the overlap in the C contents of
199 the Gagnone rocks with the Almirez chlorite harzburgites (**Figs. 1A, 2B**), the lack of the hydrated precursors
200 of the Gagnone metaperidotites prevents evaluation of whether C was lost, retained, or gained during
201 antigorite and chlorite destabilization. In fact, if the serpentinites from the Iberian margin or from the
202 Apennine are considered as hydrated precursors for the Gagnone metaperidotites (**Fig. 3A**), both C loss and
203 C retention could have occurred. Despite this unresolved conundrum, the serpentinites and the Gagnone
204 metaperidotites display notable C enrichment compared with concentrations in primitive and depleted mantle
205 (**Fig. 1A**), suggesting that surficial C acquired by exchange with ocean waters and/or with subduction fluids
206 can be transported to great depths in subduction zones.

207 As reported in **Fig 1B**, C from the Gagnone metaperidotites is to varying degrees in the form of
208 reduced C (TOC, **Table 1**) with TOC/TC ranging between 0.28 to 0.85, similar to ratios of chlorite
209 harzburgites and serpentinites for which data have previously been presented (e.g., Almirez, Voltri Massif,
210 Alt et al., 2012a, 2012b). Because significant amounts of carbonaceous materials (e.g., graphite) were not
211 detected in the Gagnone samples during petrographic investigation, we propose that the reduced C in our
212 samples may derive from micro-inclusions in the high-*P* minerals. However, the unusually high TOC values
213 for samples MG304 92-2 and MG163 09-07 (7666 and 2093 ppm, respectively), even when compatible with
214 TOC of several serpentinites from the Iberian margin with up to 4245 ppm (Schwarzenbach et al., 2013),
215 indicate either an underestimation of the TIC component or sample contamination affecting the TC data. The
216 homogeneity of the TC content and isotopic results for each replicate sample, together with their
217 compatibility with previously published data, appears to argue against a contribution of C contamination due
218 to sample treatment prior or during the analyses. Considering that the determination of the TIC content is
219 dependent on the reaction time with phosphoric acid (see Collins et al., 2015), it is possible that the amounts
220 of CO₂ analyzed did not represent 100% yields, leading to an underestimation of the TIC content for the C-
221 rich samples (see **Appendix A** for further details).

222 The negative $\delta^{13}\text{C}_{\text{TC}}$ values of the Gagnone metaperidotites are comparable to those of oceanic and
223 subduction zone serpentinites (**Fig. 2A**). The $\delta^{13}\text{C}_{\text{TOC}}$ values for the Gagnone metaperidotites (from -27.8 to-

224 26.0‰) are, in particular, similar to serpentinites from the Iberian margin (from -28.3 to -24.9‰;
225 Schwarzenbach et al., 2013). As shown in **Fig. 2A**, the $\delta^{13}\text{C}_{\text{TC}}$ of the hydrated ultramafic rocks can be
226 attributed to mixing of seawater-derived carbonate ($\delta^{13}\text{C} = -1\text{‰}$) with reduced C (close to $\delta^{13}\text{C} = -25\text{‰}$).
227 Moreover, the $\delta^{13}\text{C}$ values of organic compounds extracted from oceanic serpentinites from the Lost City
228 hydrothermal system fall between -26.6 and -25.8‰ (Delacour et al., 2008), values comparable to the
229 $\delta^{13}\text{C}_{\text{TOC}}$ of the Gagnone metaperidotites. The origin for such reduced C in serpentinites (biogenic *vs.*
230 abiogenic) is a matter of debate (e.g., Ménez et al., 2012; Sforza et al., 2018). Experimental work has shown
231 that hydrocarbons and other organic compounds strongly depleted in ^{13}C ($\delta^{13}\text{C}_{\text{TOC}} \approx -50\text{‰}$) can be produced
232 at oceanic conditions by reduction of CO_x via abiotic hydrothermal processes via an aqueous Fisher-Tropsch
233 Type reaction (McCollom and Seewald, 2006).

234 Although the low $\delta^{13}\text{C}_{\text{TC}}$ and $\delta^{13}\text{C}_{\text{TOC}}$ of the Gagnone metaperidotites can be derived from water-rock
235 interaction on the seafloor, exchange with subduction-zone metamorphic fluids sourced by the country
236 metasediments might also have contributed to their ^{13}C -depleted signatures. As demonstrated in previous
237 studies (Cannaò et al., 2015; Scambelluri et al., 2014) the elemental and isotopic compositions of the
238 Gagnone metaperidotites retain clear evidence of their interaction with fluids originating from, or previously
239 equilibrated with, nearby metasedimentary rocks. Their C isotope compositions could potentially have been
240 altered by the same fluid-rock interaction along the subduction interface. The Gagnone metasedimentary
241 rock analyzed in this study has $\delta^{13}\text{C}_{\text{TC}} = -24.4 \text{‰}$ and $\delta^{13}\text{C}_{\text{TOC}} = -27.0 \text{‰}$, values lower than those of the
242 metaperidotites, with a C concentration of about 300 ppm (**Fig. 2A**). Thus, devolatilization reactions
243 experienced by the host (meta)sedimentary rocks could have provided C with a strongly fractionated isotopic
244 composition contributing to the lowering of the originally oceanic $\delta^{13}\text{C}$ of the metaperidotites (**Fig. 2A**).
245 Discriminating among these scenarios is not straightforward; however, previous evidence for exchange of
246 the metaperidotites with the nearby metasedimentary rocks (Cannaò et al., 2015; Scambelluri et al., 2014)
247 certainly hints at the possibility of some C isotope exchange among these lithologies during subduction.

248 Another way to affect the C isotope composition of subducted ultramafic rocks is represented by
249 carbonate reduction driven by subduction fluids, a process that favours ^{13}C fractionation in the residual
250 carbonates (i.e., $\delta^{13}\text{C}_{\text{TIC}} > 0\text{‰}$) and produces reduced C phases (e.g., graphite, methane) with negative $\delta^{13}\text{C}$
251 (Galvez et al., 2013; Vitale Brovarone et al., 2017). This process could be responsible for the negative

252 $\delta^{13}\text{C}_{\text{TOC}}$ of the Gagnone metaperidotites. However, the $\delta^{13}\text{C}_{\text{TIC}}$ and $\delta^{18}\text{O}_{\text{TIC}}$ values of the Gagnone
253 metaperidotites are inconsistent with such a process having occurred. **Figure 4** shows the possible trends in
254 carbonate C-O isotope compositions during interaction with sedimentary fluids and during progressive
255 devolatilization under both oxidizing and reducing conditions. The majority of the Gagnone samples fall on a
256 trend of $\delta^{13}\text{C}_{\text{TIC}}$ depletion and $\delta^{18}\text{O}_{\text{TIC}}$ enrichment via exchange with sediment-derived fluids. In contrast, the
257 magnesite-bearing chlorite harzburgite with highest TC and heaviest $\delta^{13}\text{C}_{\text{TC}}$ (sample MG304 92-2) may
258 record CO_2 -loss from seafloor-ophicalcarbonate by progressive devolatilization at oxidized conditions, resulting
259 in decrease in $\delta^{13}\text{C}$ with subtle decrease in $\delta^{18}\text{O}$ (e.g., Collins et al., 2015). Given these arguments, the
260 reduced C hosted in the Gagnone metaperidotites was likely inherited from seafloor processes and the
261 changes in $\delta^{13}\text{C}_{\text{TIC}}$ were mostly due to decarbonation and re-equilibration with sediment-derived fluids. The
262 degrees of decarbonation and interaction by metasedimentary fluids recorded by Gagnone metaperidotites
263 are related to the amounts of inorganic/oxidized and reduced C. Thus, alternatively, the negative $\delta^{13}\text{C}_{\text{TOC}}$
264 signatures of the Gagnone samples could reflect precipitation of C-bearing phases from isotopically light
265 (i.e., reduced) fluids. The – at least transient – achievement of reducing conditions has recently been
266 proposed for the Gagnone rocks (Piccoli et al., 2019). The lack of carbonate phases in the garnet
267 metaperidotites limits our complete understanding of how and to what extent this change in the redox
268 condition contributes to the isotope evolution of carbonates.

269 For sample MG304 92-2, which contains magnesite as a part of the high-*P* mineral assemblage
270 (Scambelluri et al., 2014), and assuming TOC is present as graphite, the resulting $\Delta^{13}\text{C}_{\text{TIC-TOC}}$ of +15.4‰
271 allows to calculate an equilibrium temperature of about 380 °C (Golyshev, 1981; Scheele and Hoefs, 1992),
272 in contrast with the higher peak temperature of ~700°C estimated for these rocks (Scambelluri et al., 2014).
273 The temperature calculated seemingly demonstrates that the TIC and TOC are not in isotopic equilibrium, as
274 was reported by Alt et al. (2012) for the Almirez chlorite harzburgites.

275 The chemical exchange processes documented for the Gagnone ultramafic rocks could serve as
276 proxies for the mass transfer that occurs between slabs and serpentized supra-subduction forearc mantle.
277 Possible drag-down of such materials with hybrid geochemical signatures to greater depths (e.g., van Keken
278 et al., 2011) could contribute to the production of geochemical anomalies in the deep mantle (e.g., Kendrick
279 et al., 2018; Scambelluri et al., 2019).

280

281 **5.2. Deep nitrogen recycling**

282 Data for N concentrations in ultramafic rocks are scarce and largely limited to pure serpentinites
283 (Halama et al., 2012; Philippot et al., 2007) and mica-bearing ultramafic rocks in mélange terranes (Bebout,
284 1997). Larger numbers of data have been published for the AOC and sediments and their metamorphosed
285 equivalents (e.g., Bebout et al., 2013; Bebout and Fogel, 1992; Busigny et al., 2003; Halama et al., 2010; Li
286 et al., 2007; Philippot et al., 2007; Sadofsky and Bebout, 2003). In both pelitic and mafic systems, N is
287 incorporated mostly in K-bearing minerals as NH_4^+ . Nitrogen is fixed into mantle rocks during peridotite
288 alteration and serpentinization on the ocean floor, a process that results in enrichment in bulk N, to up to 10
289 ppm, relative to concentrations in the mantle (about 2 ppm; **Fig. 1A**). However, in oceanic serpentinites, no
290 clear correlation between N concentration and degree of serpentinization has been observed (Philippot et al.,
291 2007) and N concentrations of serpentinites from low grade (oceanic) to high-*P* conditions show no
292 significant decrease during prograde subduction-zone metamorphism (**Fig. 3B**). The de-serpentinized
293 chlorite harzburgites from Almirez have N concentrations (average = 7.4 ± 8.9 ppm) similar to those of their
294 high-*P* serpentinite protoliths, suggesting that, as for C, N is not appreciably fractionated into the fluid phase
295 during antigorite dehydration (Halama et al., 2012). The Gagnone metaperidotites have N concentrations
296 higher than those in the serpentinites (**Figs. 1A and 3B**). On average, the Gagnone chlorite harzburgites
297 contain 24 to 38 ppm of N, i.e., up to 3 to 5 times more N than their Almirez counterparts. The Gagnone
298 garnet peridotites have the highest N contents of 40 to 74 ppm, i.e., from 3 to 44 times higher than in
299 Almirez chlorite harzburgites and from 12 to 22 times higher than in the low-grade serpentinites from the
300 Northern Apennine (Italy). We suggest that the high N concentrations of the Gagnone metaperidotites can be
301 related to their subduction history and may reflect the interaction with the host metasedimentary rocks,
302 which have been shown to be an important N supplier in a number of previously-studied subduction zone
303 settings (see Bebout, 1997; Halama et al., 2017). Because N (as NH_4^+) shows geochemical behavior similar
304 to that of the LILEs, positive linear correlations commonly exist between N concentrations and those of K_2O ,
305 Rb and Cs (Busigny and Bebout, 2013). During burial of crustal rocks, NH_4^+ can be released by continuous
306 metamorphic reactions leading to decrease of the N/LILEs ratios. This feature was documented for the
307 Catalina Schists (USA), which experienced considerable loss of N in the high-grade units during

308 devolatilization reactions (e.g., N/K₂O from >200 in low-grade units to <100 in high-grade units; Bebout and
309 Fogel, 1992). The Gagnone metasedimentary rock has relatively low N concentration (33 ppm) and has a
310 bulk N/K₂O ratio of 11.3. This is consistent with the partial release of N during prograde devolatilization.

311 The mineral repositories for N in hydrated ultramafic rocks are not yet fully identified. Several
312 studies have concluded that the residency of N in the chlorite's crystal lattice is unlikely and that, in this
313 mineral, N resides in sealed voids and cracks produced during serpentinization and other subsequent
314 dehydration reactions (Halama et al., 2012; Philippot et al., 2007). Alternatively, any N present could be a
315 mixture of that in the rock residue and N₂ in fluid inclusions that experienced loss of H⁺ due to leakage at
316 oxidized conditions (Halama et al., 2012). This latter mechanism was also proposed to explain the retention
317 of noble gas in high-*P* ultramafic rocks (Kendrick et al., 2011). In both types of metaperidotites, N (as well
318 as C) could also be hosted in inclusions trapped in high-*P* minerals (Scambelluri et al., 2015). In such cases,
319 these inclusions could act as major reservoirs contributing to refertilization of the deep mantle.

320 It is worth noting that, among the Gagnone metaperidotites, the garnet-bearing rocks display the
321 higher N concentrations. Because the chlorite and garnet metaperidotites from this locality experienced
322 similar subduction histories (Scambelluri et al., 2014) the difference in their N concentration could be related
323 to the presence of amphibole and clinopyroxene in the garnet peridotites. Amphibole is a K-bearing mineral
324 and may host N (as NH₄⁺) as a substitute for the LILEs (e.g., Busigny and Bebout, 2013). Therefore, K-
325 bearing amphibole (up to 0.23 wt.% in Gagnone) may play a major role in the storage of N in ultramafic
326 systems at high-*P* conditions. However, the destabilization of amphibole above 3 GPa and at high-*T* could
327 result in a partial release of the N. Along with amphibole, the coupled substitution (Ca²⁺)_{M2} + (Mg²⁺)_{M1} ⇌
328 (NH₄⁺)_{M2} + (Cr³⁺, Al³⁺)_{M1} in clinopyroxene can contribute to N storage in ultramafic rocks (Watenphul et al.,
329 2010). Consequently, part of the N stored in garnet metaperidotites like those at Gagnone can be transferred
330 to depths beyond those at which amphibole is stable.

331 The N concentrations presented in this paper are at least one order of magnitude higher than those
332 presented in the literature (e.g., Halama et al., 2012). Great heterogeneity in the N concentrations in such
333 rocks can be envisioned and the role of serpentinites in the global N subduction input may be significantly
334 underestimated due the scarcity of datasets. For example, using the average N concentration measured for
335 the Gagnone chlorite harzburgites, the N flux contributed by hydrated ultramafic rocks can increase of 8%

336 and to a maximum of 60% (equal to 3.4 and 68.3 mol/year $\times 10^9$ of N) depending on the volume of
337 serpentized slab mantle considered (cases A and C in Halama et al., 2012). Here, it is worth noting that our
338 higher N estimates refer to rocks embedded in the plate interface subduction mélanges where they are
339 potentially enriched in N from nearby, dehydrating (meta)sediments. The hydration of supra-subduction
340 mantle in forearc region via slab-derived, N-bearing fluids during prograde metamorphism could produce
341 layers of Gagnone-like wedge serpentinites with anomalously higher N concentrations. This could be the
342 case for the wedge-derived antigorite-serpentinites of the ultrahigh-*P* Tso Moriri unit (NW Himalaya)
343 containing up to 45 ppm of N (**Fig. 3B**) as the result of interaction with fluid sourced from subducted marine
344 sediments (Pagé et al., 2018). The formation of 1 to 3 km-thick layers of serpentized forearc mantle
345 (Bostock et al., 2002; Kawakatsu and Watada, 2010) could store up to 10.6 and 31.8 mol/year $\times 10^9$ of N,
346 respectively, by assuming an a convergence rate of 0.05 cm/year and a total arc length of 44000 km (Halama
347 et al. 2012 and reference therein). The downward dragging of such materials could convey this important N-
348 rich reservoir into the upper mantle and contribute to its N inventory.

349

350 **5.3. Implications for diamond genesis**

351 An intriguing debate related to crustal recycling into the deep mantle regards the involvement of
352 subduction-derived C (and N) in the genesis of diamond (e.g., Cartigny, 2005). The C isotope distribution of
353 diamonds show a dominant peak where almost 70% of diamonds analyzed so far falls in a narrow $\delta^{13}\text{C}$
354 interval between -8 and -2‰ (**Fig. 5**), i.e., overlapping with the C isotope composition of the mantle
355 (Cartigny et al., 2014). However, worldwide, diamonds cover a much larger range of $\delta^{13}\text{C}$ interval between -
356 38.5 and +5.0‰ (Cartigny, 2005; see **Fig. 5**). The lower values are thought to represent signatures of reduced
357 C recycled in AOC and sediments. Nonetheless, several authors suggest that the contribution of recycled
358 materials is minimal and that the negative $\delta^{13}\text{C}$ (i.e., lower than mantle range) can be explained by a process
359 of isotopic fractionation prior to and/or during diamond growth (Cartigny, 2005). Preservation of the
360 primordial C isotope heterogeneity in the mantle acquired during Earth's accretion, and not homogenized by
361 convection processes, is another hypothesis that can explain the $\delta^{13}\text{C}$ variability of diamonds (Deines et al.,
362 1993). Despite such controversial scenarios arising from C isotope systematics, diamonds often incorporate
363 N in the form of molecular impurities providing information regarding the residence of volatiles in the

364 mantle (Cartigny et al., 2014). Because N is an atmophile element, its abundance in the mantle presumably
365 decreased during Earth's degassing over geological times, with concomitant increase of the N budgets hosted
366 in surficial reservoirs (Marty, 2012). The high N concentrations in diamonds thus appear to require N-rich
367 materials recycled to depth. In these recycled reservoirs (crustal and sedimentary), N is enriched in heavy
368 ^{15}N (relative to Earth's atmosphere, in large part due to biological processes), and the $\delta^{15}\text{N}$ of these rocks can
369 further increase as a result of subduction-related metamorphic reactions depending on the prograde
370 metamorphic P - T paths (Bebout et al., 2013; Bebout and Fogel, 1992; Busigny et al., 2003). The sum of the
371 above processes increases the isotopic gap between the recycled materials and the average mantle signature
372 ($\delta^{15}\text{N}_{\text{AIR}} = -5 \pm 2\text{‰}$). A complex and poorly understood relationship exists between light C and heavy N
373 isotopic signatures, therefore the correlation between recycled reduced C isotope signature and crustal-
374 derived N in diamonds is not always straightforward (Cartigny, 2005).

375 Ferropericlase and ringwoodite inclusions in diamond associated with H_2O -bearing fluids, present as
376 tiny films surrounding the inclusions (Nimis et al., 2016), support a process of subduction recycling of
377 volatiles down to the transition zone and into the lower mantle (Palot et al., 2016; Pearson et al., 2014).
378 Therefore, the idea that subducted oceanic slabs are involved in the genesis of deep, lower-mantle diamonds
379 is gaining some acceptance (Nestola et al., 2018): in this respect, the genesis of blue B-bearing diamonds in
380 the lower mantle has been linked to recycling of serpentinized materials (Smith et al., 2018). The fate of
381 dense, deserpentinized mantle rocks, such as those in the Gagnone metaperidotite suite, is to be buried and
382 enter the deep mantle. Along this pathway, these rocks can reach the depth of diamond formation in poorly-
383 defined regions of the mantle where they can impose geochemical signatures acquired during their oceanic
384 and subduction-zone metamorphic history. We propose that, as a whole, the Gagnone metaperidotites are
385 capable of introducing to the deep mantle C with a strongly fractionated $\delta^{13}\text{C}$ signature that could contribute
386 to the C isotopic heterogeneity reflected in diamonds (**Fig. 5**). The $\delta^{13}\text{C}$ fingerprints of the garnet-bearing
387 metaperidotites overlap those of diamonds ranging from about -20 to -14‰, whereas the chlorite
388 harzburgites from Gagnone, showing a wider range of $\delta^{13}\text{C}$ (see **Table 1** and **Fig. 2**), partially overlap the
389 lower end of the dominant $\delta^{13}\text{C}$ signature of diamonds (**Fig. 5**). Therefore, we propose that the Gagnone
390 metaperidotites could represent a source for diamonds with low $\delta^{13}\text{C}$ where a simple fractionation model
391 with initial $\delta^{13}\text{C}$ mantle value of -5‰ cannot provide an explanation (Cartigny, 2005). The range of $\delta^{13}\text{C}$ of

392 peridotitic diamonds from the Jagersfontein (South Africa; $\delta^{13}\text{C}$ range from -18.9 to -24.4‰; Deines et al.,
393 1991) and Orapa (Botswana; $\delta^{13}\text{C}$ range from -4.2 to -18.9‰; Deines et al., 1993) kimberlites appear to be
394 reasonably explained by our proposed scenario. Peridotitic diamonds are generally characterized by low N
395 concentrations (about 200 ppm on average; Cartigny, 2005) that match with concentrations in the Gagnone
396 metaperidotites and other serpentinites (**Figs. 1A** and **3B**). In this study we do not report the N isotope
397 composition of the Gagnone metaperidotites, however, previous work performed by Halama et al. (2012) for
398 the chlorite harzburgites of the Almirez complex suggests that the $\delta^{15}\text{N}_{\text{AIR}}$ of ultramafic rocks recycled into
399 the mantle is about $+3 \pm 2\%$. This range is similar to that reported for the peridotitic diamonds worldwide
400 (Cartigny, 2005).

401 The deep subduction of the Gagnone metaperidotites is also a viable mechanism to transfer
402 incompatible element signatures acquired during oceanic and subduction evolution into the mantle. Recent
403 mass-balance calculations provided by Scambelluri et al. (2019) highlight that, after the antigorite
404 dehydration, a significant part of the FMEs budget of the initial serpentinites, particularly B, is still trapped
405 in the produced secondary peridotites. The fractionated C isotope composition of the Gagnone
406 metaperidotites, coupled with their relatively high B concentrations (2.4 to 8.9 ppm, Cannà et al., 2015)
407 make them a potential end-member reservoir that could provide the geochemical components required for
408 the genesis of blue B-bearing diamonds (Smith et al., 2018). **Figure 6** show the overlap in the $\delta^{13}\text{C}$ and the B
409 concentrations of the blue B-bearing diamonds and the Gagnone metaperidotites reservoir. Although the
410 Gagnone rocks are representative of ultramafic rocks evolved at the top of the slab and could have
411 experienced unusual subduction evolution, the slab-derived chlorite harzburgites from the Almirez massif
412 are characterized by comparable B enrichment (Harvey et al., 2014) and depletion in ^{13}C -isotope (Alt et al.,
413 2012a), overlapping the compositions of the Gagnone metaperidotites (**Fig. 6**). This similarity suggests that
414 the mechanism of B and volatile transfer to depth by slab-derived metaperidotites could provide the required
415 geochemical ingredients required to form blue B-bearing diamonds. Smith and co-authors (2018) proposed
416 that the transfer of volatiles and incompatible elements like B into the lower mantle in the ultramafic system
417 occurs via the stabilization of dense hydrous magnesium silicates (DHMSs) prior to antigorite dehydration.
418 This transformation ensures the production of hydrous diamond-forming fluids at the great depths (Harte,
419 2010) required for diamond formation. However, the release of volatiles and incompatible elements during

420 slab burial strongly depends on the thermal setting of the individual subduction zone, which dictates the
421 devolatilization histories in slabs (e.g., Bebout et al., 1999; Bebout and Fogel, 1992; Cannaò and Malaspina,
422 2018; Syracuse et al., 2010; van Keken et al., 2011). **Figure 7** shows the P - T paths of top-slab and slab-
423 Moho for warm (Central Cascadia) and cold (Kamchatka) subduction zones (Syracuse et al., 2010) along
424 with the stability fields of major hydrous minerals in the ultramafic system (Cannaò and Malaspina, 2018
425 and reference therein). According to the above P - T trajectories, formation of secondary peridotites such as
426 the Gagnone rocks (green and red stars in **Fig. 7**) would have occurred in a relatively warm subduction zone.
427 The transformation from antigorite to DHMSs (e.g., Phase-A, 10Å-Phase) occurs only in the lower part of
428 the coolest slabs (e.g., Kamchatka, Kurile, Aleutian and NE Japan). This relationship indicates that the
429 formation of Gagnone-like metaperidotites would have been more frequent in warmer subduction zone
430 geothermal regime such as those thought to have been active during the early Earth's history (e.g., Ernst,
431 1972). Excluding amphibole and chlorite, which dehydrate at relatively low P (**Fig. 7**), all other rock-
432 forming minerals of the metaperidotites are considered nominally anhydrous (NAMs – nominally anhydrous
433 minerals) and therefore unable to provide the fluid phase required for diamond genesis. However, olivine,
434 pyroxenes, and garnet incorporate H as complex point defects in their mineral structures at the level of ppm
435 of equivalent H₂O (e.g., Beran, 2006; Férot and Bolfan-Casanova, 2012). Recent estimates of the amount of
436 H₂O carried to depth by deserpentinized slab materials via NAMs fix the concentrations at up to 110 ppm
437 (Padrón-Navarta and Hermann, 2017). Even more H₂O is estimated to be stored in NAMs in secondary
438 peridotites from wedge origin (up to 2200 ppm; Padrón-Navarta and Hermann, 2017). In the light of this,
439 Gagnone-like metaperidotites from both slab and wedge derivation could potentially transport sufficient C-
440 O-H volatile components to depth to form diamonds.

441 Uncertainty remains regarding the partitioning of C, N, B, and other trace elements in mineral phases
442 stabilized at still higher pressure, in transition zone and lower mantle, limiting our understanding of the fate
443 of these elements in the even deeper mantle. As for the pyroxenes, olivine is stable at upper mantle
444 conditions (Stixrude and Lithgow-Bertelloni, 2007), but its burial into the mantle is affected by
445 deformation(s) that could potentially influence its role as a geochemical carrier. Our current knowledge of
446 the behavior of olivine (and pyroxenes) at P - T conditions compatible with that of the lowermost part of the
447 upper mantle, the transition zone and the lower mantle, is based on consideration of changes in physical

448 properties aimed at understanding of Earth's seismic velocity structure. We know much less about the
449 chemical behavior of the deep mantle, in particular the fractionation of trace elements during: (1) the olivine
450 to wadsleyite to ringwoodite transitions (e.g., Kerschhofer et al., 2000); (2) the B-type to C-type olivine
451 fabric transition (e.g., Katayama and Karato, 2006); (3) the fate of fluid-related inclusions hosted in olivine
452 at increasing pressure and during the above phase transitions. Similarly, little is known about the ability of
453 DHMSs to store B and other incompatible elements in their structure and thus serve as the main carriers of B
454 into the mantle sources of blue B-bearing diamonds (Smith et al., 2018). The olivine to wadsleyite to
455 ringwoodite phase transitions could result in at least partial release of the elements and volatiles required for
456 diamond formation.

457

458 **6. Conclusions**

459 The antigorite breakdown at subduction-zones transforms serpentinites into secondary peridotites
460 that are injected to depth inside the mantle. This process impacts the deep C, N and incompatible element
461 recycling and contributes to development of geochemical heterogeneities in the Earth's mantle. Our study
462 can be summarized as follow:

- 463 • Carbon concentrations of the chlorite harzburgites and the garnet peridotites are comparable
464 to those of serpentinites from oceanic and subduction environments. The high variability of
465 [C] shown by oceanic serpentinites, and the lack of the hydrated precursors for the Gagnone
466 metaperidotites, make it difficult to determine whether significant C was released during
467 dehydration processes at high-*P*.
- 468 • Nitrogen concentrations of the Gagnone metaperidotites are higher than those of both non-
469 subducted oceanic serpentinites and deeply subducted serpentinites and fit well within the
470 range for concentrations for high-*P* serpentinites of wedge origins from the Himalayas. This
471 similarity suggests that the N concentrations in the Gagnone' metaperidotites were increased
472 as the result of interaction with the surrounding metasedimentary rocks during prograde
473 subduction zone metamorphism.
- 474 • The relatively low $\delta^{13}\text{C}$ of the chlorite- and garnet-bearing metaperidotites ($\delta^{13}\text{C}_{\text{TC}}$ between -
475 17.8 to -12.2‰) likely reflect an oceanic imprint involving mixing between seawater-

476 derived carbonate and a reduced C source. However, due to the complex subduction
477 evolution affecting the Gagnone metaperidotites, partial re-equilibration of their $\delta^{13}\text{C}_{\text{TC}}$
478 fingerprints with that of the surrounding metasedimentary rocks ($\delta^{13}\text{C}_{\text{TC}} = -24.4\%$) cannot
479 be discounted. The $\delta^{13}\text{C}_{\text{TC}}$ of -7.2% for the magnesite-bearing chlorite harzburgite could
480 reflect some decarbonation during subduction zone metamorphism at oxidized conditions.

481 • We speculate that the low $\delta^{13}\text{C}$ of the Gagnone metaperidotites, coupled with their
482 enrichment in B, could make these rock suitable contributors to the genesis of blue B-
483 bearing diamond in the lower mantle. We propose that this geochemical signature can be
484 transported to depth by metaperidotites generated not only in slab and slab-interface settings,
485 but also in mantle wedges.

486 Our results highlight that subduction of secondary peridotites evolved along the slab-mantle interface
487 is a viable mechanism to inject volatiles into the deep mantle, particularly in hotter geothermal regime such
488 as the ones active during the early Earth's history.

489

490 **Acknowledgements**

491 EC acknowledges funding from the Italian Society of Mineralogy and Petrology (SIMP) for support
492 his visiting at the Lehigh University with the “Borsa di Studio per l'estero 2015” and the Italian MIUR for
493 funding the PRIN program 2017ZE49E7 to MS. Funding for the inorganic C-O stable isotope work came
494 from USA-NSF grant EAR-1119264 (to GEB). Constructive reviews by J. Alt and an anonymous reviewer,
495 and editorial handling by Editor T. Mather, greatly improved the presentation of the manuscript and are
496 much appreciated.

497

498 **Figure captions**

499 **Figure 1. (A)** Carbon and nitrogen concentrations (in ppm) for the metaperidotites of Cima di Gagnone. The
500 light blue box represents the range of C and N concentrations for actual and former oceanic serpentinites and
501 high-*P* subducted serpentinites (Alt et al., 2012b; Delacour et al., 2008; Halama et al., 2012; Philippot et al.,
502 2007; Schwarzenbach et al., 2013). The dashed black box represents the range of C and N concentrations for
503 the chlorite harzburgites of Cerro del Almirez, Spain (Alt et al., 2012a; Halama et al., 2012). Values of

504 primitive and depleted mantle (PM and DM, respectively) are reported for comparison (McDonough and
505 Sun, 1995; Salters and Stracke, 2004). **(B)** Correlation between Total C and Total Inorganic Carbon of the
506 Cima di Gagnone metaperidotites. The dashed lines represent variable ratios of total C vs. total inorganic C.
507 Chlorite harzburgites with unusually high TOC content (MG304 92-2 and MG163 09-07) are indicated with
508 a black dot inside the symbol.

509
510 **Figure 2. (A)** The Total Carbon (TC, ppm) vs. $\delta^{13}\text{C}_{\text{TC}}$ of the Cima di Gagnone metaperidotites are compared
511 with oceanic ophicarbonates rocks from the Atlantis Massif (Delacour et al., 2008) and serpentinites from
512 the Iberian Margin (ODP Legs149 and 173) and Apennine Bracco unit (Schwarzenbach et al., 2013). The
513 dashed red line represents the mixing line between organic carbon (150 ppm, $\delta^{13}\text{C} = -26 \text{‰}$) and seawater
514 carbonate (2 wt.%, $\delta^{13}\text{C} = -1 \text{‰}$) reservoirs (Alt et al., 2012a). The $\delta^{13}\text{C}$ range of dissolved organic C (-26.6
515 to -25.8 ‰) is evidenced by the light black box (Delacour et al., 2008). Potential trend of decarbonation is
516 from Alt et al. (2012b). The value of the Gagnone metasediment is also reported for comparison. **(B)**
517 Comparison between the TC concentration (in ppm – logarithmic scale) and $\delta^{13}\text{C}_{\text{TC}}$ of the Cima di Gagnone
518 metaperidotites and pure oceanic and high-*P* serpentinites as well as equivalent high-*P* chlorite harzburgites
519 from Apennine low temperature, high-*P* serpentinites from Voltri Massif (Alt et al., 2012b) and from Cerro
520 del Almirez , Spain (Alt et al., 2012a). The Iberian and other Apennine Bracco serpentinites are from
521 Schwarzenbach et al. (2013). Chlorite harzburgites with unusually high TOC content (MG304 92-2 and
522 MG163 09-07) are indicated with a black dot inside the symbol.

523
524 **Figure 3.** Loss of Ignition content (LOI - wt.%) vs. Total Carbon (in ppm – **A**), Nitrogen (in ppm – **B**) and
525 $\delta^{13}\text{C}_{\text{TC}}$ (‰ – **C**) of the Gagnone metaperidotites. For comparison the values of the high-*P* serpentinites and
526 chlorite harzburgites from Cerro del Almirez and low temperature and high-*P* serpentinites from Northern
527 Apennine and Erro-Tobbio, respectively, are reported (Alt et al., 2012a; Halama et al., 2012). Nitrogen and
528 LOI contents of high-*P* serpentinites of wedge origin from the Himalayan orogen are also reported in (B)
529 (Pagé et al., 2018). The boxes in **(A)** and **(C)** report the field of the LOI vs. TC and $\delta^{13}\text{C}_{\text{TC}}$, respectively, of
530 the Iberian ODP Leg 149 and Apennine Bracco serpentinites (TC and $\delta^{13}\text{C}_{\text{TC}}$ from Schwarzenbach et al.,
531 2013; LOI contents are arbitrary fixed between 10 and 12 wt.% as no values are reported in the literature).

532 Chlorite harzburgites with unusually high TOC content (MG304 92-2 and MG163 09-07) are indicated with
533 a black dot inside the symbol.

534
535 **Figure 4.** C-O isotope composition of inorganic C from the Cima di Gagnone metaperidotites compared with
536 the field of oceanic and subducted ophicarbonates (e.g., Cannà et al., 2020, and references therein). Arrows
537 depict general trends of the processes able to modify the isotope signatures of inorganic C: progressive
538 devolatilization at both oxidized and reduced conditions (Galvez et al., 2013; Vitale-Brovarone et al., 2017)
539 and interaction with sedimentary fluids (Collins et al., 2015). Chlorite harzburgites with unusually high TOC
540 content (MG304 92-2 and MG163 09-07) are indicated with a black dot inside the symbol.

541
542 **Figure 5.** Relative frequency (in %) of the $\delta^{13}\text{C}$ signature of natural diamonds (Cartigny et al., 2014)
543 compared with the data of the metaperidotites of Cima di Gagnone (CdG) studied here. The range of the C
544 isotopic composition of the depleted mantle is reported for comparison (Deines, 2002).

545
546 **Figure 6.** $\delta^{13}\text{C}$ isotopic signatures vs. B contents (ppm) of the Gagnone metaperidotites (Cannà et al.,
547 2015), Almirez chlorite harzburgites (Harvey et al., 2014; Alt et al., 2012a) and the depleted mantle (Deines,
548 2002; Marschall et al., 2017) that may represent the end-member reservoirs for the genesis of the blue B-
549 bearing diamonds from the Earth's lower mantle (Gaillou et al., 2012). Note that most of the B content in
550 diamonds fall in the lower part of the box (below 1 ppm). Chlorite harzburgites with unusually high TOC
551 content (MG304 92-2 and MG163 09-07) are indicated with a black dot inside the symbol.

552
553 **Figure 7.** Pressure and temperature path for both warm (Central Cascadia) and cold (Kamchatka) top slab
554 (continuous lines) and slab-Moho (dotted lines) thermal settings (Syracuse et al., 2010) over the stability
555 field of key hydrous minerals in ultramafic system (antigorite, chlorite, talc, amphibole and Phase-A). The
556 development of secondary peridotites (i.e., Gagnone-like rocks) occurs in warm subduction zones (e.g., C.
557 Cascadia) and atop the slab in cold subduction thermal settings (e.g., Kamchatka). The deep transport of
558 bond water in DHMS occur by the stabilization of Phase-A at the expense of antigorite only in the lower part

559 of the cold slabs (e.g., Kamchatka). The red and green stars represent the peak conditions of the garnet- and
560 chlorite-bearing Gagnone metaperidotites, respectively (Scambelluri et al., 2014).

561

562 **References**

563

564 Alt, J.C., Garrido, C.J., Shanks, W.C.C., Turchyn, A., Padrón-Navarta, J.A., López Sánchez-Vizcaíno, V.,
565 Gómez Pugnaire, M.T., Marchesi, C., Sánchez-Vizcaíno, V.L., Pugnaire, M.T.G., 2012a. Recycling of
566 water, carbon, and sulfur during subduction of serpentinites: A stable isotope study of Cerro del
567 Almirez, Spain. *Earth Planet. Sci. Lett.* 327, 50–60. <https://doi.org/10.1016/j.epsl.2012.01.029>

568 Alt, J.C., Shanks, W.C.C., Crispini, L., Gaggero, L., Schwarzenbach, E.M., Früh-Green, G.L., Bernasconi,
569 S.M., 2012b. Uptake of carbon and sulfur during seafloor serpentinization and the effects of subduction
570 metamorphism in Ligurian peridotites. *Chem. Geol.* 322–323, 268–277.
571 <https://doi.org/10.1016/j.chemgeo.2012.07.009>

572 Alt, J.C., Teagle, D.A.H., 1999. The uptake of carbon during alteration of ocean crust 10.1016/S0016-
573 7037(99)00123-4 : *Geochimica et Cosmochimica Acta* | ScienceDirect.com. *Geochim. Cosmochim.*
574 *Acta* 63, 1527–1535. [https://doi.org/10.1016/S0016-7037\(99\)00123-4](https://doi.org/10.1016/S0016-7037(99)00123-4)

575 Bebout, G.E., 2014. Treatise on Geochemistry, in: *Analytical Geochemistry/Inorganic Instrument Analysis*.
576 Elsevier, pp. 703–747. <https://doi.org/10.1016/B978-0-08-095975-7.01401-7>

577 Bebout, G.E., 2007. Metamorphic chemical geodynamics of subduction zones. *Earth Planet. Sci. Lett.* 260,
578 373–393. <https://doi.org/10.1016/j.epsl.2007.05.050>

579 Bebout, G.E., 1997. Nitrogen isotope tracers of high-temperature fluid-rock interactions: Case study of the
580 Catalina Schist, California. *Earth Planet. Sci. Lett.* 151, 77–90. [https://doi.org/10.1016/S0012-
581 821X\(97\)00117-9](https://doi.org/10.1016/S0012-821X(97)00117-9)

582 Bebout, G.E., Agard, P., Kobayashi, K., Moriguti, T., Nakamura, E., 2013. Devolatilization history and trace
583 element mobility in deeply subducted sedimentary rocks: Evidence from Western Alps HP/UHP suites.

584 Chem. Geol. 342, 1–20. <https://doi.org/10.1016/j.chemgeo.2013.01.009>

585 Bebout, G.E., Fogel, M.L., 1992. Nitrogen-isotope compositions of metasedimentary rocks in the Catalina
586 Schist, California: Implications for metamorphic devolatilization history. *Geochim. Cosmochim. Acta.*
587 [https://doi.org/10.1016/0016-7037\(92\)90363-N](https://doi.org/10.1016/0016-7037(92)90363-N)

588 Bebout, G.E., Penniston-Dorland, S.C., 2016. Fluid and mass transfer at subduction interfaces-The field
589 metamorphic record. *Lithos.* <https://doi.org/10.1016/j.lithos.2015.10.007>

590 Bebout, G.E., Ryan, J.G., Leeman, W.P., Bebout, A.E., 1999. Fractionation of trace elements by subduction
591 zone metamorphism effect of convergent margin thermal evolution. *Earth Planet. Sci. Lett.* 171, 63–81.

592 Becker, H., 1993. Garnet peridotite and eclogite Sm-Nd mineral ages from the Lepontine dome (Swiss
593 Alps): New evidence for Eocene high-pressure metamorphism in the central Alps. *Geology* 21, 599–
594 602.

595 Beran, A., 2006. Water in Natural Mantle Minerals II: Olivine, Garnet and Accessory Minerals. *Rev.*
596 *Mineral. Geochemistry* 62, 169–191. <https://doi.org/10.2138/rmg.2006.62.8>

597 Bostock, M.G., Hyndman, R.D., Rondenay, S., Peacock, S.M., 2002. An inverted continental Moho and
598 serpentinization of the forearc mantle. *Nature* 417, 536–8.

599 Busigny, V., Ader, M., Cartigny, P., 2005. Quantification and isotopic analysis of nitrogen in rocks at the
600 ppm level using sealed tube combustion technique : A prelude to the study of altered oceanic crust 223,
601 249–258. <https://doi.org/10.1016/j.chemgeo.2005.08.002>

602 Busigny, V., Bebout, G.E., 2013. Nitrogen in the silicate earth: Speciation and isotopic behavior during
603 mineral-fluid interactions. *Elements.* <https://doi.org/10.2113/gselements.9.5.353>

604 Busigny, V., Cartigny, P., Philippot, P., Ader, M., Javoy, M., 2003. Massive recycling of nitrogen and other
605 fluid-mobile elements (K, Rb, Cs, H) in a cold slab environment: evidence from HP to UHP oceanic
606 metasediments of the Schistes Lustrés nappe (western Alps, Europe). *Earth Planet. Sci. Lett.* 215, 27–
607 42. [https://doi.org/10.1016/S0012-821X\(03\)00453-9](https://doi.org/10.1016/S0012-821X(03)00453-9)

608 Cannaò, E., Agostini, S., Scambelluri, M., Tonarini, S., Godard, M., 2015. B, Sr and Pb isotope
609 geochemistry of high-pressure Alpine metaperidotites monitors fluid-mediated element recycling
610 during serpentinite dehydration in subduction mélange (Cima di Gagnone, Swiss Central Alps).
611 *Geochim. Cosmochim. Acta* 163, 80–100. <https://doi.org/10.1016/j.gca.2015.04.024>

612 Cannaò, E., Malaspina, N., 2018. From oceanic to continental subduction : Implications for the geochemical
613 and redox evolution of the supra-subduction mantle 14.
614 <https://doi.org/10.1130/GES01597.1/4457636/ges01597.pdf>

615 Cannaò, E., Scambelluri, M., Bebout, G.E., Agostini, S., Pettke, T., Godard, M., Crispini, L., 2020.
616 Ophicarbonates evolution from seafloor to subduction and implications for deep-Earth C cycling. *Chem.*
617 *Geol.* <https://doi.org/10.1016/j.chemgeo.2020.119626>

618 Cartigny, P., 2005. Stable Isotopes and the Origin of Diamond. *Elements* 1, 79–84.
619 <https://doi.org/10.2113/gselements.1.2.79>

620 Cartigny, P., Palot, M., Thomassot, E., Harris, J.W., 2014. Diamond Formation: A Stable Isotope
621 Perspective. *Annu. Rev. Earth Planet. Sci.* 42, 699–732. [https://doi.org/10.1146/annurev-earth-042711-](https://doi.org/10.1146/annurev-earth-042711-105259)
622 [105259](https://doi.org/10.1146/annurev-earth-042711-105259)

623 Collins, N.C., Bebout, G.E., Angiboust, S., Agard, P., Scambelluri, M., Crispini, L., John, T., 2015.
624 Subduction zone metamorphic pathway for deep carbon cycling : II . Evidence from HP / UHP
625 metabasaltic rocks and ophicarbonates. *Chem. Geol.* 412, 132–150.
626 <https://doi.org/10.1016/j.chemgeo.2015.06.012>

627 Cook-Kollars, J., Bebout, G.E., Collins, N.C., Angiboust, S., Agard, P., 2014. Subduction zone metamorphic
628 pathway for deep carbon cycling: I. Evidence from HP/UHP metasedimentary rocks, Italian Alps.
629 *Chem. Geol.* 386, 31–48. <https://doi.org/10.1016/j.chemgeo.2014.07.013>

630 Deines, P., 2002. The carbon isotope geochemistry of mantle xenoliths 58, 247–278.

631 Deines, P., Harris, J.W., Gurney, J.J., 1993. Depth-related carbon isotope and nitrogen concentration
632 variability in the mantle below the Orapa kimberlite, Botswana, Africa. *Geochim. Cosmochim. Acta.*

633 [https://doi.org/10.1016/0016-7037\(93\)90390-I](https://doi.org/10.1016/0016-7037(93)90390-I)

634 Deines, P., Harris, J.W., Gurney, J.J., 1991. The carbon isotopic composition and nitrogen content of
635 lithospheric and asthenospheric diamonds from the Jagersfontein and Koffiefontein kimberlite, South
636 Africa. *Geochim. Cosmochim. Acta* 55, 2615–2625. [https://doi.org/10.1016/0016-7037\(91\)90377-H](https://doi.org/10.1016/0016-7037(91)90377-H)

637 Delacour, A., Früh-Green, G.L., Bernasconi, S.M., Schaeffer, P., Kelley, D.S., 2008. Carbon geochemistry
638 of serpentinites in the Lost City Hydrothermal System (30°N, MAR). *Geochim. Cosmochim. Acta* 72,
639 3681–3702. <https://doi.org/10.1016/j.gca.2008.04.039>

640 Ernst, W.G., 1972. Occurrence and mineralogic evolution of blueschist belts with time. *Am. J. Sci.* 272,
641 657–668. <https://doi.org/10.2475/ajs.272.7.657>

642 Evans, B.W., Trommsdorff, V., 1978. Petrogenesis of garnet lherzolite, Cima di Gagnone, Lepontine Alps.
643 *Earth Planet. Sci. Lett.* 40, 333–348.

644 Evans, B.W., Trommsdorff, V., Richter, W., 1979. Petrology of an eclogite-metarodingite suite at Cima di
645 Gagnone, Ticino, Switzerland. *Am. Mineral.* 64, 15–31.

646 Férot, A., Bolfan-Casanova, N., 2012. Water storage capacity in olivine and pyroxene to 14GPa:
647 Implications for the water content of the Earth's upper mantle and nature of seismic discontinuities.
648 *Earth Planet. Sci. Lett.* 349–350, 218–230. <https://doi.org/10.1016/j.epsl.2012.06.022>

649 Gaillou, E., Post, J.E., Rost, D., Butler, J.E., 2012. Boron in natural type IIb blue diamonds: Chemical and
650 spectroscopic measurements. *Am. Mineral.* 97, 1–18. <https://doi.org/10.2138/am.2012.3925>

651 Galvez, M.E., Martinez, I., Beyssac, O., Benzerara, K., Agrinier, P., Assayag, N., 2013. Metasomatism and
652 graphite formation at a lithological interface in Malaspina (Alpine Corsica, France). *Contrib. to*
653 *Mineral. Petrol.* 166, 1687–1708. <https://doi.org/10.1007/s00410-013-0949-3>

654 Golyshev, S.I., 1981. Fractionation of stable oxygen and carbon isotopes in carbonate systems. *Geokhimiya*
655 10, 1427–1441.

656 Guillot, S., Schwartz, S., Reynard, B., Agard, P., Prigent, C., 2015. Tectonic significance of serpentinites.

657 Tectonophysics 646, 1–19. <https://doi.org/10.1016/j.tecto.2015.01.020>

658 Halama, R., Bebout, G.E., John, T., Scambelluri, M., 2012. Nitrogen recycling in subducted mantle rocks
659 and implications for the global nitrogen cycle. *Int. J. Earth Sci.* 1–19. <https://doi.org/10.1007/s00531->
660 012-0782-3

661 Halama, R., Bebout, G.E., John, T., Schenk, V., 2010. Nitrogen recycling in subducted oceanic lithosphere :
662 The record in high- and ultrahigh-pressure metabasaltic rocks. *Geochim. Cosmochim. Acta* 74, 1636–
663 1652. <https://doi.org/10.1016/j.gca.2009.12.003>

664 Halama, R., Bebout, G.E., Marschall, H.R., John, T., 2017. Fluid-induced breakdown of white mica controls
665 nitrogen transfer during fluid–rock interaction in subduction zones. *Int. Geol. Rev.* 59, 702–720.
666 <https://doi.org/10.1080/00206814.2016.1233834>

667 Harte, B., 2010. Diamond formation in the deep mantle: the record of mineral inclusions and their
668 distribution in relation to mantle dehydration zones. *Mineral. Mag.* 74, 189–215.
669 <https://doi.org/10.1180/minmag.2010.074.2.189>

670 Harvey, J., Garrido, C.J., Savov, I.P., Agostini, S., Padrón-Navarta, J.A., Marchesi, C., Sánchez-Vizcaíno,
671 V.L., Gómez-Pugnaire, M.T., 2014. 11 B-rich fluids in subduction zones: The role of antigorite
672 dehydration in subducting slabs and boron isotope heterogeneity in the mantle. *Chem. Geol.* 376, 20–
673 30.

674 Hofmann, A.W., 2014. *Treatise on Geochemistry*, 2nd ed, The Mantle and core. Elsevier.
675 <https://doi.org/10.1016/B978-0-08-095975-7.00203-5>

676 Katayama, I., Karato, S. ichiro, 2006. Effect of temperature on the B- to C-type olivine fabric transition and
677 implication for flow pattern in subduction zones. *Phys. Earth Planet. Inter.* 157, 33–45.
678 <https://doi.org/10.1016/j.pepi.2006.03.005>

679 Kawakatsu, H., Watada, S., 2010. Seismic Evidence for Deep-Water. *Science* (80-.). 316, 1468–1471.
680 <https://doi.org/10.1126/science.1140855>

681 Kendrick, M. a., Scambelluri, M., Honda, M., Phillips, D., 2011. High abundances of noble gas and chlorine

682 delivered to the mantle by serpentinite subduction. *Nat. Geosci.* 4, 807–812.
683 <https://doi.org/10.1038/ngeo1270>

684 Kendrick, M.A., Hémond, C., Kamenetsky, V.S., Danyushevsky, L., Devey, C.W., Rodemann, T., Jackson,
685 M.G., Perfit, M.R., 2017. Seawater cycled throughout Earth’s mantle in partially serpentinized
686 lithosphere. *Nat. Geosci.* 10, 222–228. <https://doi.org/10.1038/ngeo2902>

687 Kendrick, M.A., Scambelluri, M., Hermann, J., Padrón-Navarta, J.A., 2018. Halogens and noble gases in
688 serpentinites and secondary peridotites: Implications for seawater subduction and the origin of mantle
689 neon. *Geochim. Cosmochim. Acta* 235, 285–304. <https://doi.org/10.1016/j.gca.2018.03.024>

690 Kerschhofer, L., Rubie, D.C., Sharp, T.G., McConnell, J.D.C., Dupas-Bruzek, C., 2000. Kinetics of
691 intracrystalline olivine-ringwoodite transformation. *Phys. Earth Planet. Inter.* 121, 59–76.
692 [https://doi.org/10.1016/S0031-9201\(00\)00160-6](https://doi.org/10.1016/S0031-9201(00)00160-6)

693 Li, L., Bebout, G.E., Idleman, B.D., 2007. Nitrogen concentration and $\delta^{15}\text{N}$ of altered oceanic crust
694 obtained on ODP Legs 129 and 185 : Insights into alteration-related nitrogen enrichment and the
695 nitrogen subduction budget 71, 2344–2360. <https://doi.org/10.1016/j.gca.2007.02.001>

696 Marschall, H.R., Wanless, V.D., Shimizu, N., Pogge von Strandmann, P.A.E., Elliott, T., Monteleone, B.D.,
697 2017. The boron and lithium isotopic composition of mid-ocean ridge basalts and the mantle,
698 *Geochimica et Cosmochimica Acta*. Elsevier Ltd. <https://doi.org/10.1016/j.gca.2017.03.028>

699 Marty, B., 2012. The origins and concentrations of water, carbon, nitrogen and noble gases on Earth. *Earth*
700 *Planet. Sci. Lett.* 313–314, 56–66. <https://doi.org/10.1016/j.epsl.2011.10.040>

701 McCollom, T.M., Seewald, J.S., 2006. Carbon isotope composition of organic compounds produced by
702 abiotic synthesis under hydrothermal conditions. *Earth Planet. Sci. Lett.* 243, 74–84.
703 <https://doi.org/10.1016/j.epsl.2006.01.027>

704 McDonough, W.F., Sun, S.-S., 1995. The composition of the Earth. *Chem. Geol.* 120, 223–253.

705 Ménez, B., Pasini, V., Brunelli, D., 2012. Life in the hydrated suboceanic mantle. *Nat. Geosci.* 5, 133–137.
706 <https://doi.org/10.1038/ngeo1359>

707 Meyre, C., De Capitani, C., Zack, T., Frey, M., 1999. Petrology of High-Pressure Metapelites from the
708 Adula Nappe (Central Alps, Switzerland). *J. Petrol.* 40, 199–213.
709 <https://doi.org/10.1093/etroj/40.1.199>

710 Nestola, F., Korolev, N., Kopylova, M., Rotiroti, N., Pearson, D.G., Pamato, M.G., Alvaro, M., Peruzzo, L.,
711 Gurney, J.J., Moore, A.E., Davidson, J., 2018. CaSiO₃perovskite in diamond indicates the recycling of
712 oceanic crust into the lower mantle. *Nature* 555, 237–241. <https://doi.org/10.1038/nature25972>

713 Nimis, P., Alvaro, M., Nestola, F., Angel, R.J., Marquardt, K., Rustioni, G., Harris, J.W., Marone, F., 2016.
714 First evidence of hydrous silicic fluid films around solid inclusions in gem-quality diamonds. *Lithos*
715 260, 384–389. <https://doi.org/10.1016/j.lithos.2016.05.019>

716 Padrón-Navarta, J.A., Hermann, J., 2017. A Subsolidus Olivine Water Solubility Equation for the Earth's
717 Upper Mantle. *J. Geophys. Res. Solid Earth* 122, 9862–9880. <https://doi.org/10.1002/2017JB014510>

718 Pagé, L., Hattori, K., Guillot, S., 2018. Mantle wedge serpentinites: A transient reservoir of halogens, boron,
719 and nitrogen for the deeper mantle. *Geology* 46, 883–886. <https://doi.org/10.1130/G45204.1>

720 Palot, M., Jacobsen, S.D., Townsend, J.P., Nestola, F., Marquardt, K., Miyajima, N., Harris, J.W., Stachel,
721 T., McCammon, C.A., Pearson, D.G., 2016. Evidence for H₂O-bearing fluids in the lower mantle from
722 diamond inclusion. *Lithos* 265, 237–243. <https://doi.org/10.1016/j.lithos.2016.06.023>

723 Pearson, D.G., Brenker, F.E., Nestola, F., McNeill, J., Nasdala, L., Hutchison, M.T., Matveev, S., Mather,
724 K., Silversmit, G., Schmitz, S., Vekemans, B., Vincze, L., 2014. Hydrous mantle transition zone
725 indicated by ringwoodite included within diamond. *Nature* 507, 221–4.
726 <https://doi.org/10.1038/nature13080>

727 Philippot, P., Busigny, V., Scambelluri, M., Cartigny, P., 2007. Oxygen and nitrogen isotopes as tracers of
728 fluid activities in serpentinites and metasediments during subduction. *Mineral. Petrol.* 91, 11–24.
729 <https://doi.org/10.1007/s00710-007-0183-7>

730 Piccoli, F., Hermann, J., Pettke, T., Connolly, J.A.D., Kempf, E.D., Vieira Duarte, J.F., 2019. Subducting
731 serpentinites release reduced, not oxidized, aqueous fluids. *Sci. Rep.* 9, 1–7.

732 <https://doi.org/10.1038/s41598-019-55944-8>

733 Piccoli, F., Vitale, A., Beyssac, O., Martinez, I., Ague, J.J., Chaduteau, C., 2016. Carbonation by fluid – rock
734 interactions at high-pressure conditions : Implications for carbon cycling in subduction zones. *Earth*
735 *Planet. Sci. Lett.* 1, 1–14. <https://doi.org/10.1016/j.epsl.2016.03.045>

736 Sadofsky, S.J., Bebout, G.E., 2003. Record of forearc devolatilization in low-T, high-P/T metasedimentary
737 suites: Significance for models of convergent margin chemical cycling. *Geochemistry, Geophys.*
738 *Geosystems* 4, 1–29. <https://doi.org/10.1029/2002GC000412>

739 Salters, V.J.M., Stracke, A., 2004. Composition of the depleted mantle. *Geochemistry, Geophys. Geosystems*
740 5, n/a-n/a. <https://doi.org/10.1029/2003GC000597>

741 Scambelluri, M., Bebout, G.E., Belmonte, D., Gilio, M., Campomenosi, N., Collins, N., Crispini, L., 2016.
742 Carbonation of subduction-zone serpentinite (high-pressure ophicarbonates ; Ligurian Western Alps)
743 and implications for the deep carbon cycling. *Earth Planet. Sci. Lett.* 441, 155–166.
744 <https://doi.org/10.1016/j.epsl.2016.02.034>

745 Scambelluri, M., Cannà, E., Gilio, M., 2019. The water and fluid-mobile element cycles during serpentinite
746 subduction. A review. *Eur. J. Mineral.* 1–24. <https://doi.org/10.1127/ejm/2019/0031-2842>

747 Scambelluri, M., Pettke, T., Cannà, E., 2015. Fluid-related inclusions in Alpine high-pressure peridotite
748 reveal trace element recycling during subduction-zone dehydration of serpentinitized mantle (Cima di
749 Gagnone, Swiss Alps). *Earth Planet. Sci. Lett.* 429, 45–59. <https://doi.org/10.1016/j.epsl.2015.07.060>

750 Scambelluri, M., Pettke, T., Rampone, E., Godard, M., Reusser, E., 2014. Petrology and trace element
751 budgets of high-pressure peridotites indicate subduction dehydration of serpentinitized mantle (Cima di
752 Gagnone, Central Alps, Switzerland). *J. Petrol.* 55, 459–498. <https://doi.org/10.1093/petrology/egt068>

753 Scheele, N., Hoefs, J., 1992. Carbon isotope fractionation between calcite, graphite and CO₂: an
754 experimental study. *Contrib. to Mineral. Petrol.* 112, 35–45. <https://doi.org/10.1007/BF00310954>

755 Schwarzenbach, E.M., Caddick, M.J., Petroff, M., Gill, B.C., Cooperdock, E.H.G., Barnes, J.D., 2018.
756 Sulphur and carbon cycling in the subduction zone mélange. *Sci. Rep.* 8, 1–11.

757 <https://doi.org/10.1038/s41598-018-33610-9>

758 Schwarzenbach, E.M., Früh-Green, G.L., Bernasconi, S.M., Alt, J.C., Plas, A., 2013. Serpentinization and
759 carbon sequestration: A study of two ancient peridotite-hosted hydrothermal systems. *Chem. Geol.* 351,
760 115–133. <https://doi.org/10.1016/j.chemgeo.2013.05.016>

761 Sforza, M.C., Brunelli, D., Pisapia, C., Pasini, V., Malferrari, D., Ménez, B., 2018. Abiotic formation of
762 condensed carbonaceous matter in the hydrating oceanic crust. *Nat. Commun.* 9.
763 <https://doi.org/10.1038/s41467-018-07385-6>

764 Smart, K.A., Tappe, S., Stern, R.A., Webb, S.J., Ashwal, L.D., 2016. Early Archaean tectonics and mantle
765 redox recorded in Witwatersrand diamonds. *Nat. Geosci.* 9, 255–259. <https://doi.org/10.1038/ngeo2628>

766 Smith, E.M., Shirey, S.B., Richardson, S.H., Nestola, F., Bullock, E.S., Wang, J., Wang, W., 2018. Blue
767 boron-bearing diamonds from Earth's lower mantle. *Nature* 560, 84–87.
768 <https://doi.org/10.1038/s41586-018-0334-5>

769 Stixrude, L., Lithgow-Bertelloni, C., 2007. Influence of phase transformations on lateral heterogeneity and
770 dynamics in Earth's mantle. *Earth Planet. Sci. Lett.* 263, 45–55.
771 <https://doi.org/10.1016/j.epsl.2007.08.027>

772 Syracuse, E.M., van Keken, P.E., Abers, G. a., 2010. The global range of subduction zone thermal models.
773 *Phys. Earth Planet. Inter.* 183, 73–90.

774 van Keken, P.E., Hacker, B.R., Syracuse, E.M., Abers, G. a., 2011. Subduction factory: 4. Depth-dependent
775 flux of H₂O from subducting slabs worldwide. *J. Geophys. Res.* 116, B01401.
776 <https://doi.org/10.1029/2010JB007922>

777 Vitale Brovarone, A., Martinez, I., Elmaleh, A., Compagnoni, R., Chaduteau, C., Ferraris, C., Esteve, I.,
778 2017. Massive production of abiotic methane during subduction evidenced in metamorphosed
779 ophicarbonates from the Italian Alps. *Nat. Commun.* 8, 1–13. <https://doi.org/10.1038/ncomms14134>

780 Watenphul, A., Wunder, B., Wirth, R., Heinrich, W., 2010. Ammonium-bearing clinopyroxene: A potential
781 nitrogen reservoir in the Earth's mantle. *Chem. Geol.* 270, 240–248.

782 <https://doi.org/10.1016/j.chemgeo.2009.12.003>

783

Figure 1
[Click here to download high resolution image](#)

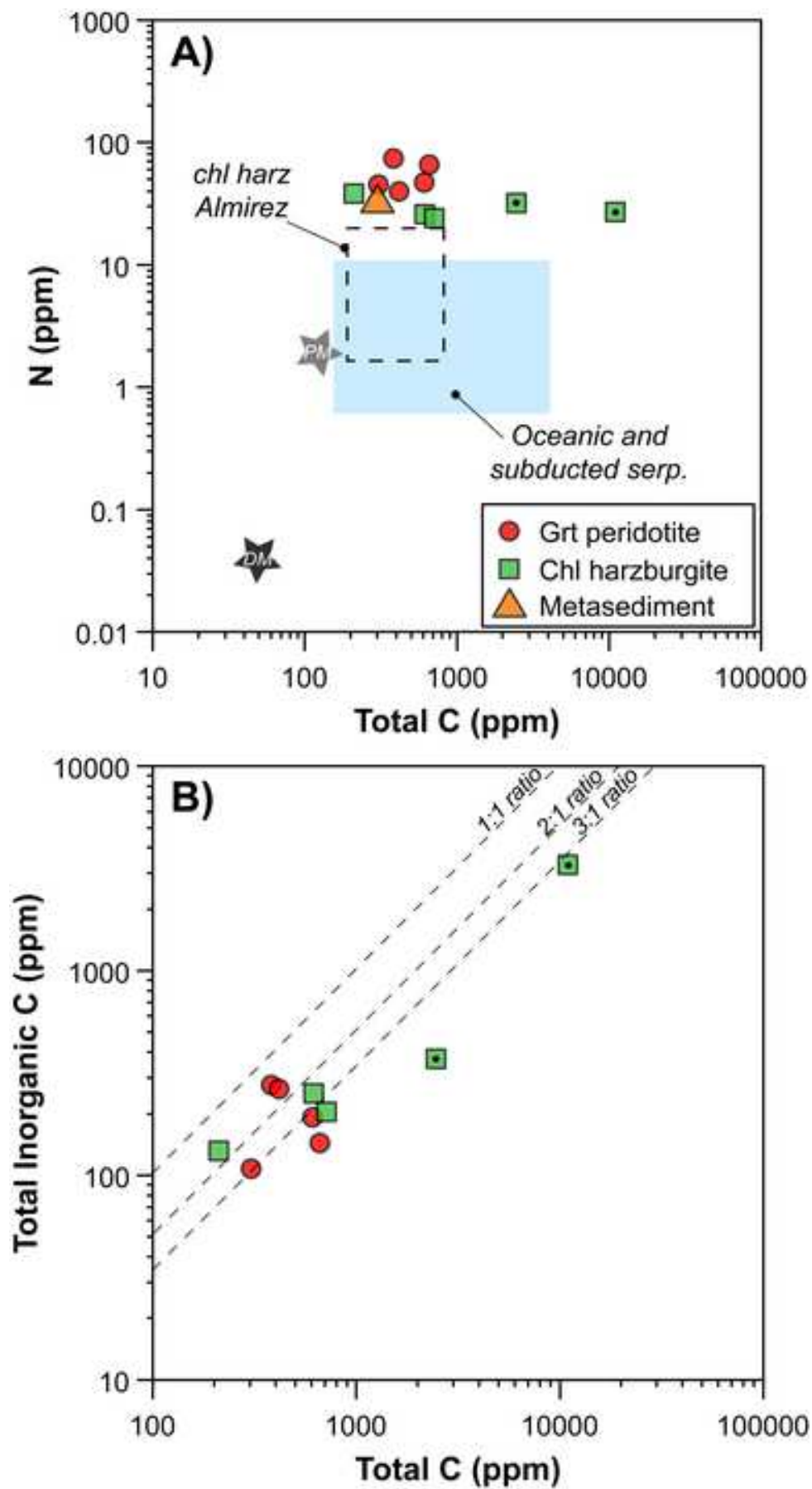


Figure 2
[Click here to download high resolution image](#)

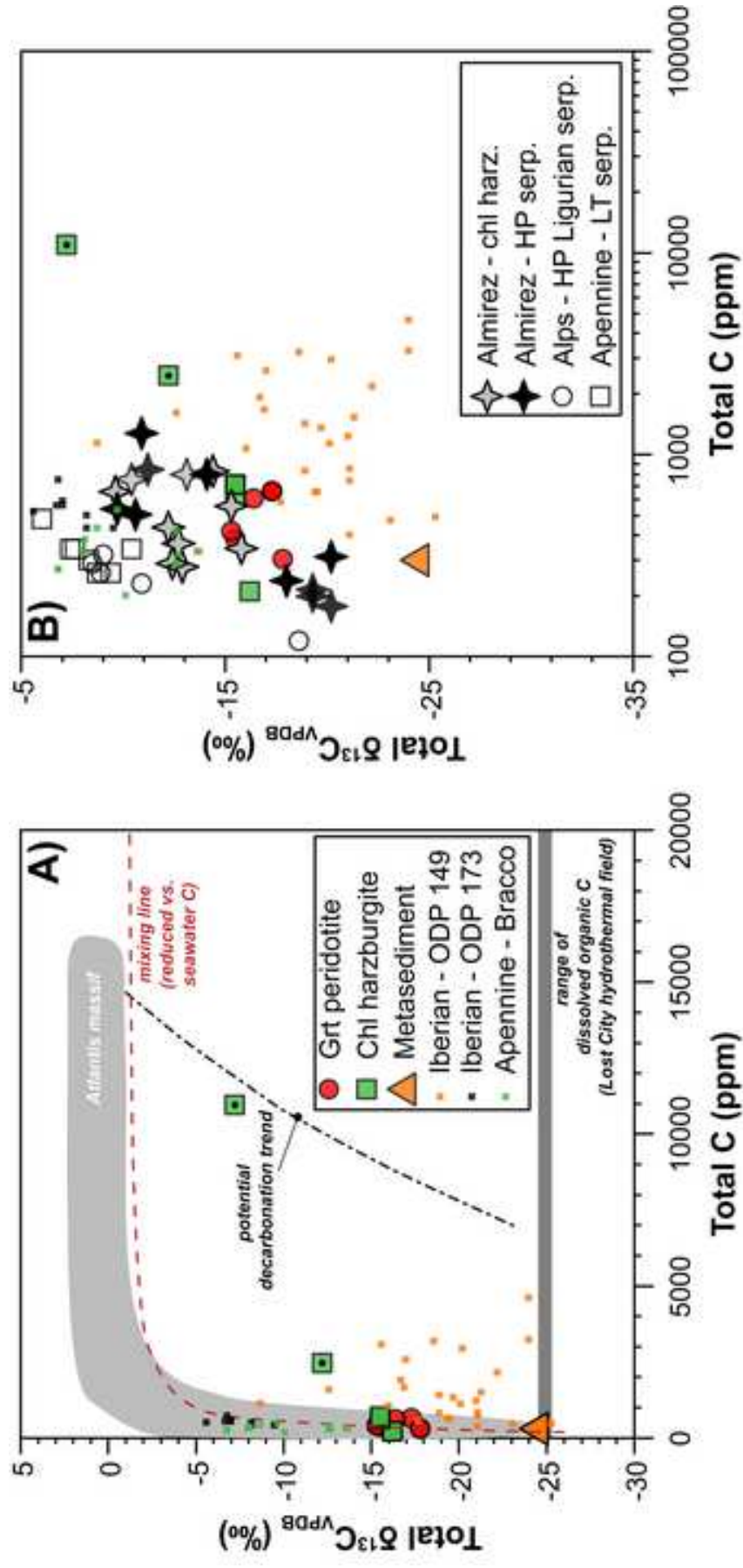


Figure 3
[Click here to download high resolution image](#)

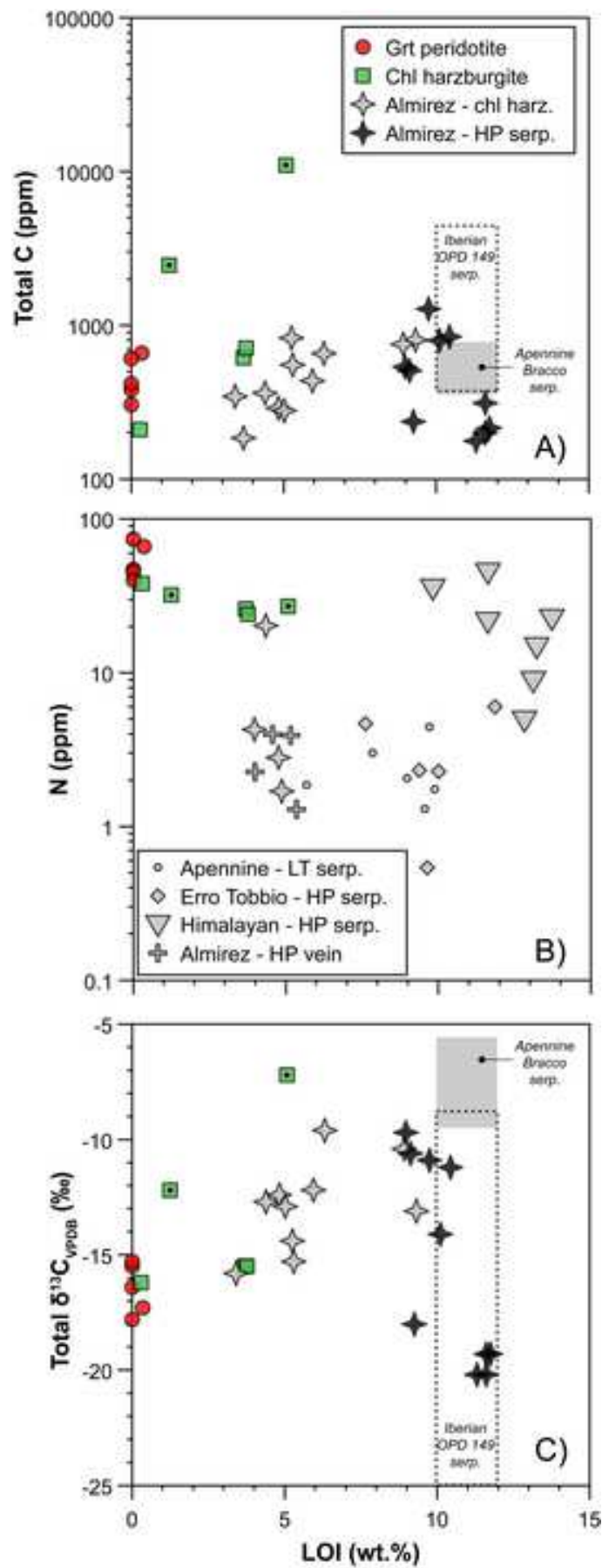


Figure 4
[Click here to download high resolution image](#)

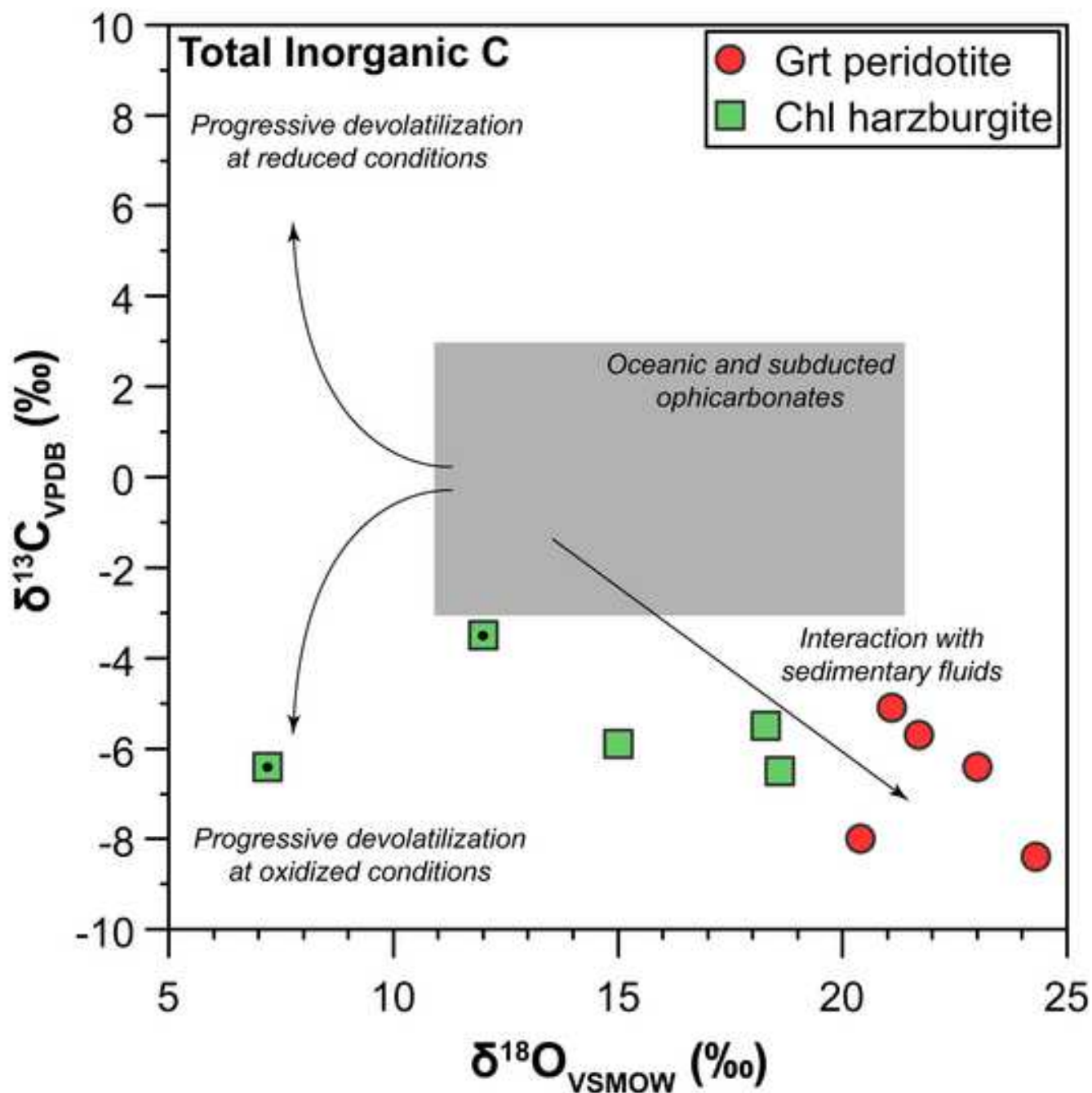


Figure 5
[Click here to download high resolution image](#)

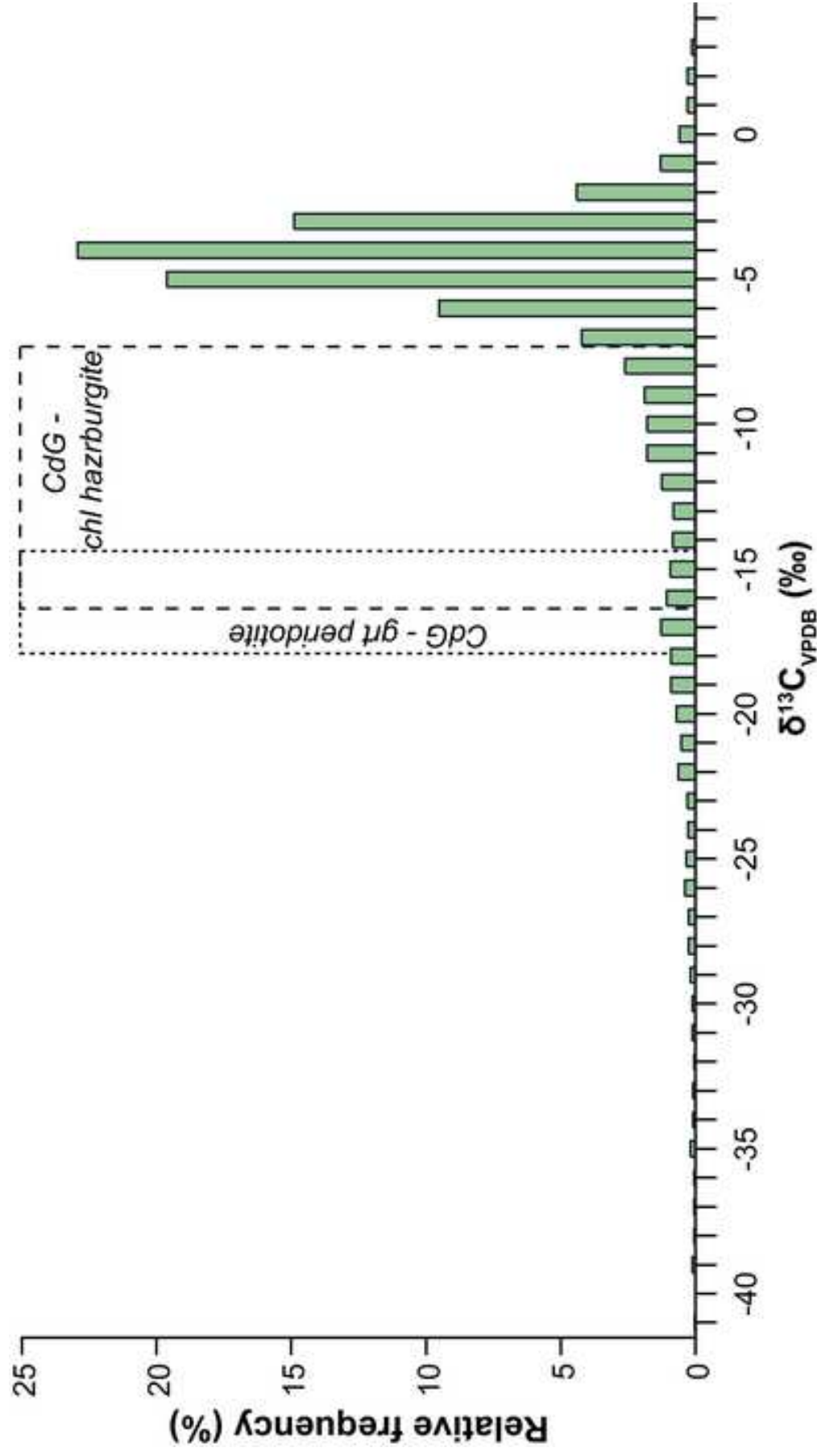


Figure 6
[Click here to download high resolution image](#)

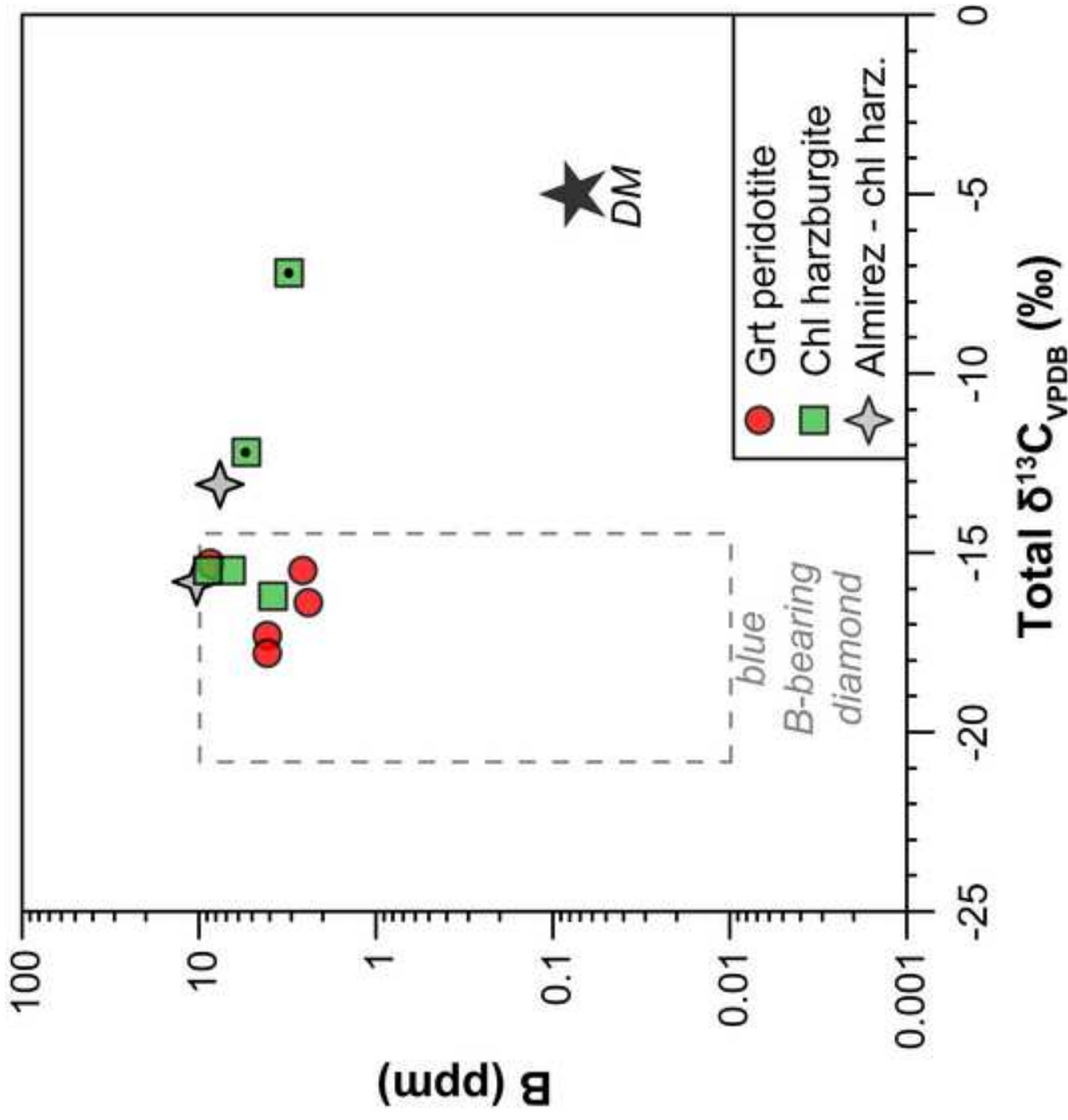


Figure 7
[Click here to download high resolution image](#)

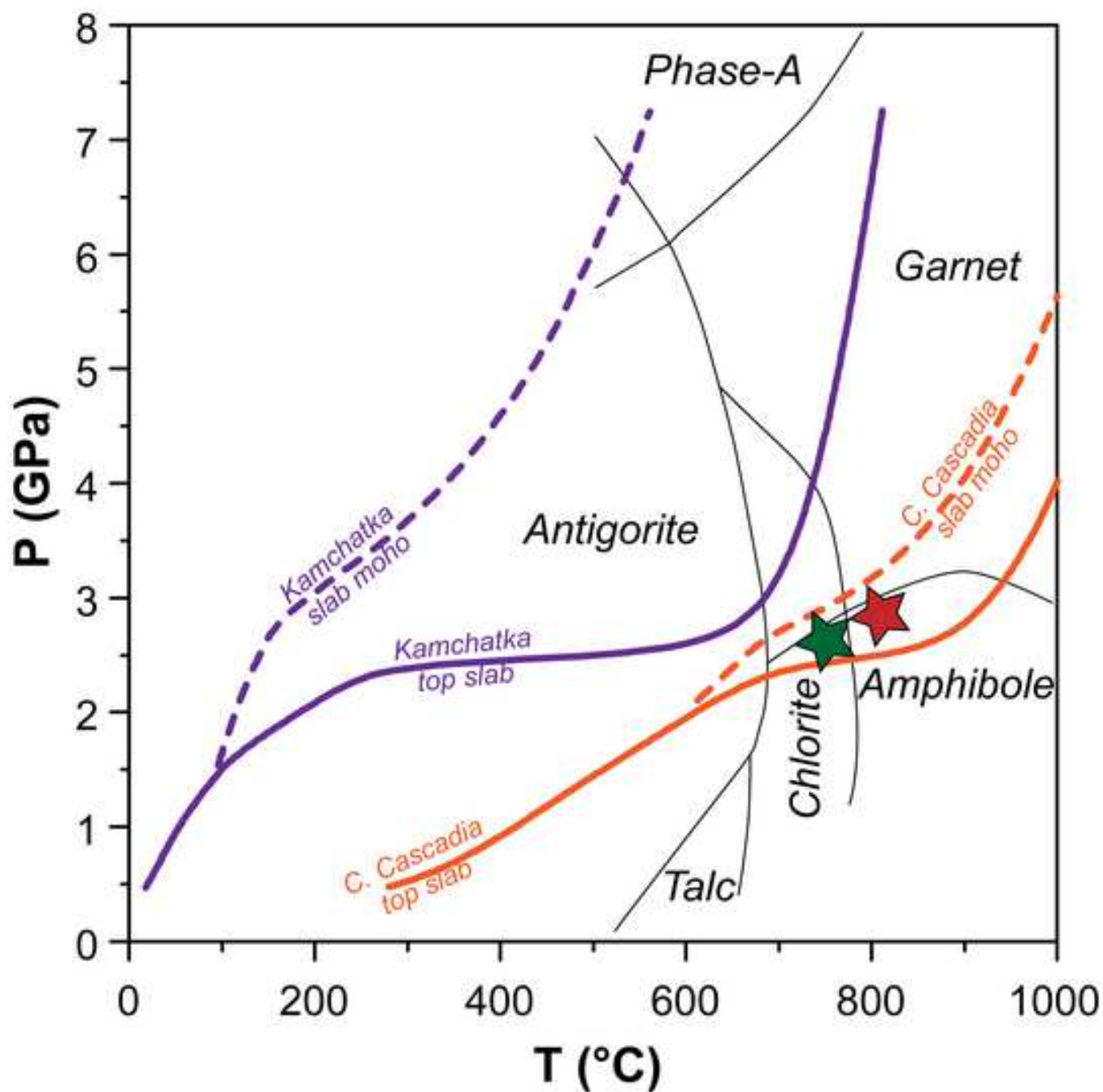


Table 1

[Click here to download Table: Table1_rev.xlsx](#)

Table 1. Nitrogen (N) and carbon (C) concentrations (in ppm) and $\delta^{13}\text{C}$ and $\delta^{18}\text{O}$ (‰) of C

	N	sd	C_{TC}	sd	C_{TIC}	^aC_{TOC}
Garnet peridotite						
MG160 4/8	66	1	659	13	144	515
MG160 09-10G	74	2	382	11	276	106
MG160 96-2	47	1	608	9	192	416
MG161 92-1	45	1	304	6	108	196
MG160 09-10	40	1	417	13	264	153
Chlorite harzburgite						
MG304 92-1	38	1	210	5	132	78
MG304 92-2	27	1	10966	307	3300 ^b	7666 ^c
MG31 09-06	26	1	616	12	252	364
MG163 09-07	32	1	2465	76	372 ^b	2093 ^c
MG163 12-03	24	1	712	18	204	508
Metasediment						
MG163 12-17	33	2	301	3	<i>nd</i>	<i>nd</i>

TC - Total Carbon; *TIC* - Total Inorganic Carbon; *TOC* - Total Organic Carbon

nd - not determined

^acalculated $\text{C}_{\text{TOC}} = \text{C}_{\text{TC}} - \text{C}_{\text{TIC}}$

^bpotential underestimated value

^cpotential overestimated value